

Blind Community Detection from Low-rank Excitations of a Graph Filter

Hoi-To Wai, Santiago Segarra, Asuman E. Ozdaglar, Anna Scaglione, Ali Jadbabaie

arXiv:1809.01485v1 [cs.SI] 5 Sep 2018

Abstract— This paper considers a novel framework to detect communities in a graph from the observation of signals at its nodes. We model the observed signals as noisy outputs of an unknown network process — represented as a graph filter — that is excited by a set of low-rank inputs. Rather than learning the precise parameters of the graph itself, the proposed method retrieves the community structure directly; Furthermore, as in *blind* system identification methods, it does not require knowledge of the system excitation. The paper shows that communities can be detected by applying spectral clustering to the low-rank output covariance matrix obtained from the graph signals. The performance analysis indicates that the community detection accuracy depends on the spectral properties of the graph filter considered. Furthermore, we show that the accuracy can be improved via a low-rank matrix decomposition method when the excitation signals are known. Numerical experiments demonstrate that our approach is effective for analyzing network data from diffusion, consumers, and social dynamics.

Index Terms— community detection, graph signal processing, low-rank matrix recovery, spectral clustering

I. INTRODUCTION

The emerging field of *network science* and availability of *big data* have motivated researchers to extend signal processing techniques to the analysis of signals defined on graphs, motivating a new area of research referred to as *graph signal processing* (GSP) [2]–[4]. As opposed to signals on time defined on a regular topology, the properties of *graph signals* are intimately related to the generally irregular topology of the graph where they are defined. The goal of GSP is to develop mathematical tools to leverage this topological structure in order to enhance our understanding of graph signals. A suitable way to capture the graph’s structure is via the so-called *graph shift operator* (GSO), which is a matrix that reflects the local connectivity of the graph and is a generalization of the time shift or delay operator in classical discrete signal processing [2]. Admissible choices for the GSO include the graph’s adjacency matrix and the Laplacian matrix. When the GSO is known, the algebraic and spectral characteristics of a given graph signal can be analyzed in an analogous way as in time-series analysis [2]. Furthermore, signal processing tools such as sampling [5], [6], interpolation [7], [8] and filtering [9], [10] can be extended to the realm of graph signals.

This work is supported by NSF CCF-BSF 1714672, an MIT IDSS seed fund, and Spanish MINECO TEC2013-41604-R. A preliminary version of this work has been presented at ICASSP 2018 in Calgary, Canada [1].

H.-T. Wai and A. Scaglione are with School of ECEE, Arizona State University, Tempe, AZ, USA. E-mails: {htwai, Anna.Scaglione}@asu.edu. S. Segarra is with Department of ECE, Rice University, TX, USA. E-mail: segarra@rice.edu. A. E. Ozdaglar is with LIDS, Massachusetts Institute of Technology, MA, USA. A. Jadbabaie is with IDSS, Massachusetts Institute of Technology, MA, USA. E-mails: {asuman, jadbabai}@mit.edu.

This paper considers an *inverse* problem in GSP where our focus is to infer information about the graph from the observed graph signals. Naturally, *graph or network inference* is relevant to network and data science, and has been studied extensively. Classical methods are based on partial correlations [11], Gaussian graphical models [12], and structural equation models [13], among others. Recently, GSP-based methods for graph inference have emerged, which tackle the problem as a system identification task. They postulate that the unknown graph is a structure encoded in the observed signals and the signals are obtained from observations of network dynamical processes defined on the graph [14], [15]. Different assumptions are put forth in the literature to aid the graph topology inference, such as smoothness of the observed signals [16]–[18], richness of the inputs to the network process [19]–[21], and partial knowledge of the network process [13], [22].

A drawback common to the prior GSP work on graph inference [16]–[21] is that they require the observed graph signals to be *full-rank*. Equivalently, the signals observed are results of a network dynamical process excited by a set of input signals that span a space with the same dimension as the number of nodes in the graph. Such assumption can be unnecessarily stringent for a number of applications, especially when the graph contains a large number of nodes. For example, whenever graph inference experiments can only be performed by exciting a few nodes on the graph (such as rumor spreading initiated by a small number of sources and the gene perturbation experiments in [23]); or the amount of data collected is limited due to cost and time constraints.

This paper addresses the aforementioned drawback by considering a less stringent assumption on the excitation model yet inferring meaningful information about the graph. We consider the graph inference problem where the observed graph signals are modeled as the outputs of an unknown network process — represented by a graph filter — excited by a set of *low-rank* input signals. Under this weaker set of assumptions, the exact inference of the underlying graph is challenging due to the lack of full observations. As such, we focus instead on inferring the *community structure* [24] of the unknown graph, *i.e.*, finding a partition of the node set into blocks or clusters. Intuitively, while our observation model is insufficient to recover the exact topology of the graph, it can recover coarser topological features. Often times, the interest is not in the complete graph, but in structures such as clusters. In particular, we propose two *blind community detection* (BlindCD) methods that do not require learning the graph topology explicitly nor knowing the dynamics governing the generation of graph signals. The first method applies spectral clustering on the sampled covariance

matrix, while the second method works under the additional assumption that the input signals are available and *boosts* the performance of the first one by leveraging a low-rank plus sparse structure in the linear transformation between the input and output signals. An important observation made in this paper is that, under the assumption that the underlying graph filter is *low-pass*, the covariance matrix of output graph signals can be viewed as a *sketch* of the graph's Laplacian which retains coarser topological features, like communities. The performance of the BlindCD methods are then analyzed and compared to the benchmark obtained by applying spectral clustering with perfect knowledge of the graph.

In addition to the theoretical results summarized above, we consider two case studies on network dynamics that model different social behaviors. We demonstrate that setting up pricing experiments in a consumers' game [25], [26] and injecting new opinions in a social system with DeGroot dynamics [27] both give rise to graph signals where the BlindCD methods can be naturally applied. Numerical experiments are performed for these models to validate our results.

Notation — We use boldface lower-case (*resp.* upper-case) letters to denote vectors (*resp.* matrices). For a vector \mathbf{x} , the notation x_i denotes its i th element and we use $\|\mathbf{x}\|_2$ to denote the standard Euclidean norm. For a matrix \mathbf{X} , the notation X_{ij} denotes its (i, j) th element whereas $[\mathbf{X}]_{i,:}$ denotes its i th row vector and $[\mathbf{X}]_{:,i}$ denotes the collection of its row vectors in \mathcal{I} . Also, $\mathcal{R}(\mathbf{X}) \subseteq \mathbb{R}^N$ denotes the range space of $\mathbf{X} \in \mathbb{R}^{N \times M}$. Moreover, $\|\mathbf{X}\|_F$ (*resp.* $\|\mathbf{X}\|_2$) denotes the Frobenius norm (*resp.* spectral norm). For a symmetric matrix \mathbf{E} , $\beta_i(\mathbf{E})$ denotes its i th largest eigenvalue. For a matrix $\mathbf{M} \in \mathbb{R}^{P \times N}$, $\sigma_i(\mathbf{M})$ denotes its i th largest singular value and $[\mathbf{M}]_K$ denotes its rank K approximation. Moreover, \mathbf{M} admits the partition $\mathbf{M} = [\mathbf{M}_K \ \mathbf{M}_{N-K}]$ where \mathbf{M}_K (*resp.* \mathbf{M}_{N-K}) denotes the matrix consisting of the *left-most* K (*resp.* *right-most* $N - K$) columns of \mathbf{M} . Similarly, $\mathbf{m} \in \mathbb{R}^N$ is partitioned into $\mathbf{m} = [\mathbf{m}_K; \mathbf{m}_{N-K}]$, where \mathbf{m}_K (*resp.* \mathbf{m}_{N-K}) consists of its *top* K (*resp.* *bottom* $N - K$) elements. For any integer K , we denote $[K] := \{1, \dots, K\}$.

II. PRELIMINARIES

We introduce basic concepts in graph signal processing and community detection that will be used throughout the paper.

A. Graph Signal Processing

Consider an undirected graph $G = (V, E, \mathbf{A})$ with N nodes such that $V = [N] := \{1, \dots, N\}$ and $E \subseteq V \times V$ is the set of edges where $(i, i) \notin E$ for all i . The graph G is also associated with a symmetric and weighted adjacency matrix $\mathbf{A} \in \mathbb{R}_+^{N \times N}$ such that $A_{ij} = A_{ji} > 0$ if and only if $(i, j) \in E$. The graph Laplacian matrix for G is defined as $\mathbf{L} := \mathbf{D} - \mathbf{A}$, where $\mathbf{D} := \text{Diag}(\mathbf{A}\mathbf{1})$ is a diagonal matrix containing the weighted degrees of G . As \mathbf{L} is symmetric and positive semidefinite, it admits the following eigendecomposition

$$\mathbf{L} = \mathbf{V} \Lambda \mathbf{V}^\top, \quad (1)$$

where $\Lambda = \text{Diag}([\lambda_1, \dots, \lambda_N])$ and λ_i is sorted in *ascending order* such that $0 = \lambda_1 \leq \lambda_2 \leq \dots \leq \lambda_N$.

A graph signal is defined as a function on the nodes of G , $f : V \rightarrow \mathbb{R}$, and can be equivalently represented as a vector $\mathbf{x} := [x_1, x_2, \dots, x_N] \in \mathbb{R}^N$, where x_i is the signal value at the i th node. The graph is endowed with a graph shift operator (GSO) \mathbf{S} that is set as the graph Laplacian, *i.e.*, $\mathbf{S} = \mathbf{L}$. Note that it is also possible to define alternative GSOs such as the adjacency matrix \mathbf{A} and its normalized versions; see [2] for an overview on the subject. Having defined the GSO, the graph Fourier transform (GFT) [2] of \mathbf{x} is given by

$$\tilde{\mathbf{x}} := \mathbf{V}^\top \mathbf{x}. \quad (2)$$

The vector $\tilde{\mathbf{x}}$ is called the *frequency* domain representation of \mathbf{x} with respect to (w.r.t.) the GSO \mathbf{S} [2], [4].

The GSO \mathbf{S} can be used to define linear graph filters. These are linear graph signal operators that can be expressed as matrix polynomials on \mathbf{S} :

$$\mathcal{H}(\mathbf{S}) := \sum_{t=0}^{T-1} h_t \mathbf{S}^t = \mathbf{V} \left(\sum_{t=0}^{T-1} h_t \Lambda^t \right) \mathbf{V}^\top, \quad (3)$$

where T is the *order* of the graph filter. Note that by the Cayley-Hamilton theorem, any matrix polynomial (even of infinite degree) can be represented using the form (3) with $T \leq N$. For a given input graph signal $\mathbf{z} \in \mathbb{R}^N$, the output of the filter is simply $\mathbf{x} = \mathcal{H}(\mathbf{S})\mathbf{z}$, and carries the classical interpretation of being a linear combination of shifted versions of the input. From an implementation perspective, a graph filter can be applied in a distributed way via $T - 1$ rounds of information exchanges between neighboring nodes, due to the locality of the shift \mathbf{S} . The graph filter $\mathcal{H}(\mathbf{S})$ may also be represented by its frequency response $\tilde{\mathbf{h}}$, defined as

$$\tilde{h}_i := h(\lambda_i) = \sum_{t=0}^{T-1} h_t \lambda_i^t. \quad (4)$$

We denote the polynomial $h(\lambda) := \sum_{t=0}^{T-1} h_t \lambda^t$ as the *generating function* of the graph filter. From (3) it follows that the frequency representations of the input and the output of a filter are related by

$$\tilde{\mathbf{x}} = \tilde{\mathbf{h}} \odot \tilde{\mathbf{z}}, \quad (5)$$

where \odot denotes the element-wise product. This is analogous to the convolution theorem for time signals.

B. Community Detection via Spectral Clustering

Given the desired number of communities K and the graph adjacency matrix \mathbf{A} , the goal of *community detection* is to find a partition of the node set V into K disjoint sets, *i.e.*, $V = \mathcal{C}_1 \cup \dots \cup \mathcal{C}_K$ where $\mathcal{C}_i \cap \mathcal{C}_j = \emptyset$ if $i \neq j$, such that the subgraph induced by each \mathcal{C}_k is densely connected while loosely connected with nodes not in \mathcal{C}_k . Each of the sets \mathcal{C}_k found is called a *community* or cluster. To this end, our goal is to search for a partition that achieves the minimum *cut* weight across the boundary between communities. A common objective is to minimize the *ratio-cut* function

$$\text{RatioCut}(\mathcal{C}_1, \dots, \mathcal{C}_K) := \sum_{k=1}^K \frac{1}{|\mathcal{C}_k|} \sum_{i \in \mathcal{C}_k} \sum_{j \in \bar{\mathcal{C}}_k} A_{ij}, \quad (6)$$

where $\bar{\mathcal{C}}_k = V \setminus \mathcal{C}_k$ is the complement of \mathcal{C}_k ; see [24] for an overview on the subject.

Clearly, the ratio-cut minimization problem is combinatorial and difficult to solve. A popular remedy is to use the convex relaxation of the problem – a method known as the *spectral clustering* [28]. To describe the method, let us define the left- K eigenmatrix of \mathbf{L} ,

$$\mathbf{V}_K := (\mathbf{v}_1 \ \mathbf{v}_2 \ \cdots \ \mathbf{v}_K) \in \mathbb{R}^{N \times K}, \quad (7)$$

where \mathbf{v}_i is the i th eigenvector of \mathbf{L} corresponding to the i th eigenvalue λ_i [cf. (1)]. The K -means method [29] is applied on the row vectors of \mathbf{V}_K , which seeks the partition $\mathcal{C}_1, \dots, \mathcal{C}_K$ that minimizes the distance of each row vector to their respective means. More precisely, we minimize

$$F(\mathcal{C}_1, \dots, \mathcal{C}_K) := \sum_{k=1}^K \sum_{i \in \mathcal{C}_k} \left\| \mathbf{v}_i^{\text{row}} - \frac{1}{|\mathcal{C}_k|} \sum_{j \in \mathcal{C}_k} \mathbf{v}_j^{\text{row}} \right\|_2^2, \quad (8)$$

where $\mathbf{v}_j^{\text{row}} := [\mathbf{V}_K]_{j,:}$ is the j th row vector of \mathbf{V}_K . Note that the minimization of $F(\cdot)$ is NP-hard in general [30]. However, efficient heuristics have been developed. For example, [31] proposed a polynomial-time algorithm that finds an $(1 + \epsilon)$ -optimal solution, $\tilde{\mathcal{C}}_1, \dots, \tilde{\mathcal{C}}_K$, to the K -means problem (8) satisfying

$$F(\tilde{\mathcal{C}}_1, \dots, \tilde{\mathcal{C}}_K) \leq (1 + \epsilon) \min_{\mathcal{C}_1, \dots, \mathcal{C}_K \subseteq V} F(\mathcal{C}_1, \dots, \mathcal{C}_K), \quad (9)$$

under some statistical assumptions on $\{\mathbf{v}_i^{\text{row}}\}_{i=1}^N$.

An important insight gained from the spectral clustering method is that only the first K eigenvectors of \mathbf{L} are required for community detection. Since $K \ll N$, this suggests that the community structure is encoded in a low-dimensional space, and enables us to retrieve the community structure even when only a set of low-rank observations is available.

III. BLIND COMMUNITY DETECTION

We consider a community detection problem in the absence of knowledge of the graph Laplacian \mathbf{S} . We observe a set of graph signals $\{\mathbf{y}^\ell\}_{\ell=1}^L$ that are collected as a result of L excitations $\{\mathbf{x}^\ell\}_{\ell=1}^L$ of an *unknown* graph filter $\mathcal{H}(\mathbf{S})$, given by

$$\mathbf{y}^\ell = \mathcal{H}(\mathbf{S})\mathbf{x}^\ell + \mathbf{w}^\ell, \quad 1 \leq \ell \leq L, \quad (10)$$

where \mathbf{w}^ℓ includes both the modeling as well as the measurement error in the data collection, which we assume is zero mean and sub-Gaussian with $\mathbb{E}[\mathbf{w}^\ell(\mathbf{w}^\ell)^\top] = \sigma_w^2 \mathbf{I}$.

The low-rank excitation model we consider is such that $\{\mathbf{x}^\ell\}_{\ell=1}^L$ belong to an R -dimensional subspace of \mathbb{R}^N with $K \leq R \ll N$, where K is the desired number of communities. In particular, we let $\mathbf{B} \in \mathbb{R}^{N \times R}$ and write

$$\mathbf{x}^\ell = \mathbf{B}\mathbf{z}^\ell. \quad (11)$$

Without loss of generality, we assume that \mathbf{z}^ℓ is a random, zero-mean, sub-Gaussian signal satisfying $\mathbb{E}[\mathbf{z}^\ell(\mathbf{z}^\ell)^\top] = \mathbf{I}$. The model above is justified when the excitation signals are controlled through a few parameters. In addition, the input covariance is given by $\mathbb{E}[\mathbf{x}^\ell(\mathbf{x}^\ell)^\top] = \mathbf{B}\mathbf{B}^\top \neq \sigma_x^2 \mathbf{I}$ such that in general, it is not spatially white even if $R = N$. In the

Algorithm 1 Blind Community Detection (BlindCD).

- 1: **Input:** Graph signals $\{\mathbf{y}^\ell\}_{\ell=1}^L$; desired number of communities K .
- 2: Compute the sample covariance $\hat{\mathbf{C}}_y$ as
$$\hat{\mathbf{C}}_y = (1/L) \sum_{\ell=1}^L \mathbf{y}^\ell(\mathbf{y}^\ell)^\top. \quad (14)$$
- 3: Find the top- K eigenvectors of $\hat{\mathbf{C}}_y$ (with the eigenvalues sorted in *descending* order). Denote the set of eigenvectors as $\hat{\mathbf{V}}_K \in \mathbb{R}^{N \times K}$.
- 4: Apply the K -means method, which seeks to optimize
$$\min_{\mathcal{C}_1, \dots, \mathcal{C}_K \subseteq V} \sum_{k=1}^K \sum_{i \in \mathcal{C}_k} \left\| \hat{\mathbf{v}}_i^{\text{row}} - \frac{1}{|\mathcal{C}_k|} \sum_{j \in \mathcal{C}_k} \hat{\mathbf{v}}_j^{\text{row}} \right\|_2^2, \quad (15)$$
where $\hat{\mathbf{v}}_i^{\text{row}} := [\hat{\mathbf{V}}_K]_{i,:} \in \mathbb{R}^K$.
- 5: **Output:** K communities $\hat{\mathcal{C}}_1, \dots, \hat{\mathcal{C}}_K$.

absence of full-rank and white excitations, it is difficult to reconstruct \mathbf{S} unless additional knowledge on $\mathcal{H}(\mathbf{S})$ is given, e.g., see [19], [22] for a related study.

We propose a *blind community detection* (BlindCD) method where we infer the community information in \mathbf{S} from the graph signals, without the need to estimate \mathbf{S} . To explain our approach, some observations are in order. The covariances of $\mathbf{x}^\ell, \mathbf{y}^\ell$ are given by

$$\begin{aligned} \mathbf{C}_x &:= \mathbb{E}[\mathbf{x}^\ell(\mathbf{x}^\ell)^\top] = \mathbf{B}\mathbf{B}^\top, \\ \mathbf{C}_y &:= \mathbb{E}[\mathbf{y}^\ell(\mathbf{y}^\ell)^\top] = \mathcal{H}(\mathbf{S})\mathbf{C}_x\mathcal{H}^\top(\mathbf{S}) + \sigma_w^2 \mathbf{I}. \end{aligned} \quad (12)$$

To simplify notation, we define $\bar{\mathbf{C}}_y := \mathcal{H}(\mathbf{S})\mathbf{C}_x\mathcal{H}^\top(\mathbf{S})$, i.e., the covariance of \mathbf{y}^ℓ in the absence of measurement error. Moreover, observe that [cf. (3), (4)]

$$\mathcal{H}(\mathbf{S})\mathbf{B} = \mathbf{V}\text{Diag}(\tilde{\mathbf{h}})\mathbf{V}^\top\mathbf{B}. \quad (13)$$

We can interpret $\mathcal{H}(\mathbf{S})\mathbf{B}$ as a *sketch* of the graph filter $\mathcal{H}(\mathbf{S})$, where \mathbf{B} is a sketch matrix to compress the right dimension from N to R . To gain insights, let us assume that the noise is small ($\sigma_w^2 \approx 0$). From (12) and (13), when the first K elements in $\tilde{\mathbf{h}}$ are non-zero and the columns of \mathbf{B} span the same space as $\text{span}\{\mathbf{v}_1, \dots, \mathbf{v}_K\}$, one can recover \mathbf{V}_K (up to a rotation) by obtaining the top- K eigenvectors of $\bar{\mathbf{C}}_y$. This intuition motivates us to detect communities by applying spectral clustering on $\bar{\mathbf{C}}_y$, as outlined in Algorithm 1.

A. Low-pass Graph Filters

Following (13) and the ensuing discussion, the performance of BlindCD depends on $\tilde{\mathbf{h}}$, the frequency response of the graph filter. In particular, a desirable situation would be one where $\tilde{\mathbf{h}}$ contains only significant entries over the first K elements; in this way, the graph filter $\mathcal{H}(\mathbf{S})$ is approximately rank K and retains all the eigenvectors required for spectral clustering. We quantify the above condition by formally introducing the notion of a *low-pass graph filter* (LPGF).

Definition 1 A graph filter $\mathcal{H}(\mathbf{S})$ is a (K, η) -LPGF if

$$\eta := \frac{\max\{|\tilde{h}_{K+1}|, \dots, |\tilde{h}_N|\}}{\min\{|\tilde{h}_1|, \dots, |\tilde{h}_K|\}} < 1, \quad (16)$$

where \tilde{h}_i is defined in (4). The LPGF is ideal if $\eta = 0$.

Note that a small η implies a ‘good’ LPGF, since $\eta \ll 1$ implies that most of the energy is concentrated in the first K frequency bins of the graph filter. In fact, as we show later in Section III-B, the low-pass coefficient η plays an important role in the performance of BlindCD.

We now survey a few graph filter designs that are LPGF and comment on their low-pass coefficients η .

Example 1 (Consensus dynamics). Consider the filter order $T < \infty$ and

$$\mathcal{H}_1(\mathbf{S}) = (\mathbf{I} - \alpha \mathbf{S})^{T-1}, \quad \alpha \in (0, 1/\lambda_N) \quad (17)$$

This filter models a discrete time consensus process after $(T-1)$ time instances on the graph [32]. In particular,

$$\eta_1 = \left(\frac{1 - \alpha \lambda_{K+1}}{1 - \alpha \lambda_K} \right)^{T-1}. \quad (18)$$

Observe that the coefficient η_1 improves exponentially with T .

Example 2 (Exponential filter). Consider $\sigma \in (0, \infty)$ and

$$\mathcal{H}_2(\mathbf{S}) = \exp(-\sigma \mathbf{S}), \quad (19)$$

The above models a process where the weight of higher powers of the graph shift decays at an exponential rate. In particular,

$$\eta_2 = \exp(-\sigma(\lambda_{K+1} - \lambda_K)), \quad (20)$$

i.e., the filter’s coefficient η_2 improves as the spectral gap $\lambda_{K+1} - \lambda_K$ increases for the graph Laplacian.

Example 3 (Single-pole IIR filter). Consider

$$\mathcal{H}_3(\mathbf{S}) = (\mathbf{I} + c^{-1} \mathbf{S})^{-1}, \quad (21)$$

for some $c > 0$. This filter is analogous to a single-pole infinite impulse response (IIR) filter in classical signal processing. Its low-pass coefficient can be bounded as

$$\eta_3 = \frac{1 + c^{-1} \lambda_K}{1 + c^{-1} \lambda_{K+1}} = 1 - c^{-1} \frac{\lambda_{K+1} - \lambda_K}{1 + c^{-1} \lambda_{K+1}}. \quad (22)$$

Observe that the coefficient $\eta_3 \approx 1$ for $\lambda_{K+1} \gg 1$ or $c \gg 1$.

An overview of graph filters and their relevant network processes can be found in [2], [4].

We conclude this subsection by characterizing the low-pass coefficient η from the properties of the generating function $h(\lambda)$. To simplify the analysis, we consider the class of filters such that $h(\lambda)$ satisfies the following assumption.

Assumption 1 The generating function $h(\lambda)$ is non-negative and non-increasing for all $\lambda \geq 0$.

Note that Assumption 1 holds for the graph filters in Examples 1 to 3. The following observation gives a bound on η using the first and second order derivatives of $h(\lambda)$.

Observation 1 Suppose that Assumption 1 holds and that $h(\lambda)$ is L_h -smooth and μ_h -strongly convex for $\lambda \in$

$[\lambda_K, \lambda_{K+1}]$, where $0 \leq \mu_h \leq L_h$. Then, the graph filter $\mathcal{H}(\mathbf{S})$ is a (K, η) -LPGF with

$$\begin{aligned} \eta &\leq 1 - \frac{1}{\tilde{h}_K} \left(\frac{\mu_h}{2} \Delta \lambda_K^2 - h'(\lambda_{K+1}) \Delta \lambda_K \right), \\ \eta &\geq 1 - \frac{1}{\tilde{h}_K} \left(\frac{L_h}{2} \Delta \lambda_K^2 - h'(\lambda_{K+1}) \Delta \lambda_K \right), \end{aligned} \quad (23)$$

where $\Delta \lambda_K := \lambda_{K+1} - \lambda_K$ is the spectral gap of \mathbf{S} .

The observation can be verified using the definitions of L_h -smooth and μ_h -strongly convex functions [33]. Note that Assumption 1 implies that $h(\lambda)$ is convex and the derivative $h'(\lambda_{K+1})$ is non-positive. Consequently, the upper bound on η depends on the spectral gap $\Delta \lambda_K$ and the magnitude of \tilde{h}_K . In particular, for a constant spectral gap, a small \tilde{h}_K leads to $\eta \approx 0$ and thus a good LPGF.

B. Performance Analysis

In this subsection, we bound the suboptimality of the communities obtained by BlindCD compared to the ‘optimal’ ones found by perfect knowledge of \mathbf{S} . Our performance metric is taken as the K -means objective function $F(\cdot)$ in (8) constructed from actual eigenvectors of \mathbf{S} . We denote by

$$F^* := \min_{\mathcal{C}_1, \dots, \mathcal{C}_K \subseteq V} F(\mathcal{C}_1, \dots, \mathcal{C}_K) \quad (24)$$

the optimal objective value. To formally state our result, let us provide a few necessary definitions. The singular value decomposition (SVD) of $\mathcal{H}(\mathbf{S})\mathbf{B}$ is given by $\overline{\mathbf{V}}\mathbf{\Sigma}\mathbf{Q}^\top$ such that $\mathbf{\Sigma} = \text{Diag}(\sigma_1, \dots, \sigma_R)$ and $\sigma_1 \geq \dots \geq \sigma_R$.

Recall that $\widehat{\mathbf{C}}_y$ is the sampled covariance of $\{\mathbf{y}^\ell\}_{\ell=1}^L$ and $\overline{\mathbf{C}}_y$ is the covariance of \mathbf{y}^ℓ in the absence of noise. The ensuing performance guarantee follows.

Theorem 1 Under the following conditions:

- 1) For some $\epsilon \geq 0$, the partition $\hat{\mathcal{C}}_1, \dots, \hat{\mathcal{C}}_K$ found by BlindCD is an $(1 + \epsilon)$ optimal solution to problem (15)¹.
- 2) $\mathcal{H}(\mathbf{S})$ is a (K, η) -LPGF [cf. Definition 1],
- 3) $\text{rank}(\mathbf{V}_K \text{diag}(\tilde{h}_K) \mathbf{V}_K^\top \mathbf{B} \mathbf{Q}_K) = K$,
- 4) $\text{rank}(\mathcal{H}(\mathbf{S})\mathbf{B}) \geq K$,
- 5) There exists $\delta > 0$ such that

$$\delta := \beta_K(\overline{\mathbf{C}}_y) - \beta_{K+1}(\overline{\mathbf{C}}_y) - \|\widehat{\mathbf{C}}_y - \overline{\mathbf{C}}_y\|_2 > 0, \quad (25)$$

where $\beta_K(\overline{\mathbf{C}}_y)$ is the K th largest eigenvalue of $\overline{\mathbf{C}}_y$.

Then,

$$\begin{aligned} &\sqrt{F(\hat{\mathcal{C}}_1, \dots, \hat{\mathcal{C}}_K)} - \sqrt{(1 + \epsilon)F^*} \\ &\leq (2 + \epsilon)\sqrt{2K} \left(\sqrt{\frac{\gamma^2}{1 + \gamma^2}} + \frac{\|\widehat{\mathbf{C}}_y - \overline{\mathbf{C}}_y\|_2}{\delta} \right), \end{aligned} \quad (26)$$

where γ is bounded by

$$\gamma \leq \eta \|\mathbf{V}_{N-K}^\top \mathbf{B} \mathbf{Q}_K\|_2 \|\mathbf{V}_K^\top \mathbf{B} \mathbf{Q}_K\|_2^{-1}. \quad (27)$$

The proof (partially inspired by [34]) can be found in Appendix A.

¹This means that the objective value obtained is at most $(1 + \epsilon)$ times the optimal value. See [31] for a polynomial-time algorithm achieving this.

Theorem 1 bounds the optimality gap for the communities found applying BlindCD compared to F^* in (24). This bound consists of the sum of two contributions. The first term is a function of γ , which in turn depends on the low-pass coefficient η of the LPGF involved as well as the alignment between the matrices \mathbf{BQ}_K and \mathbf{V}_{N-K} . From (27), the recovered communities are more accurate when: 1) the LPGF is close to ideal ($\eta \approx 0$) and 2) the distortion induced by \mathbf{B} on the relevant eigenvectors \mathbf{V}_K is minimal. The second term depends on the distance between $\widehat{\mathbf{C}}_y$ and $\overline{\mathbf{C}}_y$, capturing the combined effect of noise in the observations (via σ_w^2) as well as the finite sample size. To further control this term, if we define $\Delta := \widehat{\mathbf{C}}_y - \overline{\mathbf{C}}_y$, the next result follows.

Lemma 1 [35, Remark 5.6.3, Exercise 5.6.4] Suppose that i) $\mathbf{y}^1, \dots, \mathbf{y}^L$ are independent, and ii) they are bounded almost surely with $\|\mathbf{y}^\ell\|_2 \leq K$. Let the effective rank of \mathbf{C}_y be $r := \text{Tr}(\mathbf{C}_y)/\|\mathbf{C}_y\|_2$, then for every $c > 0$ with probability at least $1 - c$, one has that

$$\|\Delta\|_2 \leq \sigma_w + C \left(\sqrt{\frac{K^2 r \log(N/c)}{L}} + \frac{K^2 r \log(N/c)}{L} \right), \quad (28)$$

for some constant C that is independent of N, r, L, c , and σ_y .

Condition ii) in Lemma 1 is satisfied if \mathbf{y}^ℓ is sub-Gaussian and $N \gg 1$. From Lemma 1 it follows that the error converges to σ_w at the rate of $\mathcal{O}(\sqrt{rK^2 \log(N)/L})$. For our model, it can be verified that $r \approx R \ll N$, where R is the rank of \mathbf{B} and the sampling complexity is significantly reduced compared to a signal model with full-rank excitations.

We now discuss the conditions considered in Theorem 1. Notice that step 4 of BlindCD in Algorithm 1 applies K -means clustering. Thus, it is natural that the communities obtained depend on the performance of the specific K -means algorithm used. This is captured in condition 1), where a better K -means solver leads to a smaller ϵ and thus a tighter bound [cf. (26)]. Condition 2) requires that the graph filter involved is an LPGF. This natural requisite imposes that the frequency response must be higher for those eigenvectors that capture the community structure in the graph. Conditions 3) and 4) are technical requirements implying that the rank R of the excitation matrix \mathbf{B} cannot be smaller than the number of clusters K that we are trying to recover. Lastly, condition 5) imposes a restriction on the distance between the true covariance $\overline{\mathbf{C}}_y$ and the observed one $\widehat{\mathbf{C}}_y$. This condition may be violated if the spectral gap $\beta_K(\overline{\mathbf{C}}_y) - \beta_{K+1}(\overline{\mathbf{C}}_y)$ is small or, relying on Lemma 1, if the noise power σ_w^2 is large.

In a nutshell, Theorem 1 illustrates the effects that the observation noise, the finite number of observations, and the low-pass structure of the filter have on the suboptimality of the communities obtained. As discussed above, the low-pass coefficient η plays an important role in the performance of BlindCD. While η is determined by the dynamics that generates the graph signals $\{\mathbf{y}^\ell\}_{\ell=1}^L$, it is possible to improve this coefficient, as described in the next section.

IV. BOOSTED BLIND COMMUNITY DETECTION

We present a ‘boosting’ technique that extracts an improved low-pass filtered component, *i.e.*, one with a reduced coefficient η , from the observed graph signals. For the application of this technique, we shall work with graph filters satisfying Assumption 1 and consider a modified observation model where, apart from the access to the output signals $\mathbf{y}^\ell \in \mathbb{R}^N$ we also have access to the corresponding input signals $\mathbf{z}^\ell \in \mathbb{R}^R$ [cf. (10) and (11)]. As an example, this would be the case if we can design the excitation levels of R nodes and get to observe the response of the network process to this excitation.

The input-output pairs $\{\mathbf{z}^\ell, \mathbf{y}^\ell\}_{\ell=1}^L$ enable us to estimate the $N \times R$ matrix $\mathcal{H}(\mathbf{S})\mathbf{B}$ via the least square estimator

$$\mathcal{H}^* \in \arg \min_{\mathcal{H} \in \mathbb{R}^{N \times R}} \frac{1}{L} \sum_{\ell=1}^L \left\| \mathbf{y}^\ell - \hat{\mathcal{H}} \mathbf{z}^\ell \right\|_2^2, \quad (29)$$

where the solution is unique when $L \geq R$ and $\{\mathbf{z}^\ell\}_{\ell=1}^L$ spans \mathbb{R}^R . Furthermore, notice that

$$\mathcal{H}^* \approx \mathcal{H}(\mathbf{S})\mathbf{B} = \tilde{\mathcal{H}}(\mathbf{S})\mathbf{B} + \tilde{h}_N \mathbf{B}, \quad (30)$$

where we denote

$$\tilde{\mathcal{H}}(\mathbf{S}) := \mathcal{H}(\mathbf{S}) - \tilde{h}_N \mathbf{I} \quad (31)$$

with the generating function $\tilde{h}(\lambda) = h(\lambda) - \tilde{h}_N$.

The new graph filter $\tilde{\mathcal{H}}(\mathbf{S})$ is a *boosted LPGF* as it has a smaller low-pass coefficient, denoted by $\tilde{\eta}$, than the low-pass coefficient of $\mathcal{H}(\mathbf{S})$. This can be seen since (i) the magnitude of the boosted K th frequency response is reduced to $\tilde{h}_K - \tilde{h}_N$; (ii) the first and second order derivatives of $\tilde{h}(\lambda)$ are the same as $h(\lambda)$. Applying Observation 1 it follows that $\tilde{\mathcal{H}}(\mathbf{S})$ has a smaller low-pass coefficient $\tilde{\eta}$ by replacing \tilde{h}_K by $\tilde{h}_K - \tilde{h}_N$ in (23). Concretely, we observe the following example.

Example 4 (Boosted single-pole IIR filter). Consider

$$\mathcal{H}_4(\mathbf{S}) := \mathcal{H}_3(\mathbf{S}) - (1 + c^{-1} \lambda_N)^{-1} \mathbf{I}, \quad (32)$$

where $\mathcal{H}_3(\mathbf{S})$ was defined in (21) and we note that $\tilde{h}_N = (1 + c^{-1} \lambda_N)^{-1}$. We have

$$\eta_4 = \frac{\lambda_N - \lambda_{K+1}}{\lambda_N - \lambda_K} \frac{1 + c^{-1} \lambda_K}{1 + c^{-1} \lambda_{K+1}} = \left(\frac{\lambda_N - \lambda_{K+1}}{\lambda_N - \lambda_K} \right) \eta_3.$$

Obviously, $\eta_4 \ll \eta_3$ whenever $\lambda_{K+1} \gg \lambda_K$.

In general, the discussion above shows that it is possible to reduce the low-pass coefficient η significantly by adjusting the constant level of the frequency responses in graph filters. As a result, applying spectral clustering based on the top- K left singular vectors of $\tilde{\mathcal{H}}(\mathbf{S})\mathbf{B}$ will return a more accurate community detection result.

In order to estimate $\tilde{\mathcal{H}}(\mathbf{S})\mathbf{B}$ from \mathcal{H}^* as in (30), one needs, in principle, to have access to \mathbf{B} and the frequency response \tilde{h}_N . However, our goal is to obtain a boosting effect in the absence of knowledge about \mathbf{B} and \tilde{h}_N . A key towards achieving this goal is to notice that $\tilde{\mathcal{H}}(\mathbf{S})\mathbf{B}$ is close to a rank- K matrix since $\tilde{\mathcal{H}}(\mathbf{S})$ has a small low-pass coefficient $\tilde{\eta}$. Hence, for $R > K$, it follows from (30) that \mathcal{H}^* can be decomposed into a low-rank matrix and a scaled version of the sketch matrix \mathbf{B} . This motivates us to consider the noisy matrix decomposition problem proposed in [36]:

$$\begin{aligned} \min_{\hat{\mathbf{S}}, \hat{\mathbf{B}} \in \mathbb{R}^{N \times R}} \quad & \frac{1}{2} \|\mathcal{H}^* - \hat{\mathbf{S}} - \hat{\mathbf{B}}\|_{\text{F}}^2 + \kappa \|\hat{\mathbf{S}}\|_{\sigma,1} + \rho g(\hat{\mathbf{B}}) \\ \text{s.t.} \quad & g^*(\hat{\mathbf{S}}) \leq \alpha, \end{aligned} \quad (33)$$

Algorithm 2 Boosted BlindCD method.

- 1: **Input:** Graph signals and excitation signals $\{\mathbf{y}^\ell, \mathbf{z}^\ell\}_{\ell=1}^L$ and desired number of communities K .
- 2: Solve the convex optimization problem (33) and denote its solution as $(\hat{\mathbf{S}}^*, \hat{\mathbf{B}}^*)$.
- 3: Find the top- K left singular vectors of $\hat{\mathbf{S}}^*$ and denote the set of singular vectors as $\tilde{\mathbf{S}}_K \in \mathbb{R}^{N \times K}$.
- 4: Apply the K -means method on the row vectors of $\tilde{\mathbf{S}}_K$.
- 5: **Output:** K communities $\tilde{\mathcal{C}}_1, \dots, \tilde{\mathcal{C}}_K$.

where $\|\hat{\mathbf{S}}\|_{\sigma,1}$ is the trace norm of the matrix $\hat{\mathbf{S}}$, \mathcal{H}^* is a solution to (29), $\alpha, \kappa, \rho > 0$ are predefined parameters, $g(\cdot)$ is a decomposable regularizer of $\hat{\mathbf{B}}$, which is a norm chosen according to the prior knowledge on the unknown sketch matrix \mathbf{B} and $g^*(\cdot)$ is its dual norm. A few examples for choices of $g(\cdot)$ are listed below.

- *Localized excitation:* We set

$$g_1(\hat{\mathbf{B}}) = \|\text{vec}(\hat{\mathbf{B}})\|_1, \quad g_1^*(\hat{\mathbf{S}}) = \|\text{vec}(\hat{\mathbf{S}})\|_\infty. \quad (34)$$

This regularization forces the solution $\hat{\mathbf{B}}^*$ to (33) to be an element-wise sparse matrix. This corresponds to the scenario where each element of the latent variables in \mathbf{z}^ℓ excites only a few of the nodes in our graph.

- *Small number of excited nodes:* Let $\hat{\mathbf{b}}_i^{\text{row}}$ be the i th row vector of $\hat{\mathbf{B}}$. We then set

$$g_2(\hat{\mathbf{B}}) = \sum_{i=1}^N \|\hat{\mathbf{b}}_i^{\text{row}}\|_2, \quad g_2^*(\hat{\mathbf{S}}) = \max_{i=1, \dots, N} \|\hat{\mathbf{s}}_i^{\text{row}}\|_2. \quad (35)$$

This regularization is motivated by the group-sparsity formulation in [37] which forces the solution $\hat{\mathbf{B}}^*$ to (33) to be row-sparse. Notice that this is relevant when the graph filter is excited on a small number of nodes.

- *Small perturbation:* We set

$$g_3(\hat{\mathbf{B}}) = \|\hat{\mathbf{B}}\|_{\text{F}}, \quad g_3^*(\hat{\mathbf{S}}) = \|\hat{\mathbf{S}}\|_{\text{F}}. \quad (36)$$

This regularization models each entry of $\tilde{\mathbf{h}}_N \mathbf{B}$ as a Gaussian random variable of small, identical variance. This can be used when there is no prior knowledge on \mathbf{B} .

Notice that for every choice of the regularizer $g(\cdot)$ discussed, (33) is a convex problem that can be solved in polynomial time. Upon solving (33), we apply spectral clustering on the solution $\hat{\mathbf{S}}^*$ based on its top- K left singular vectors. An overview of the boosted BlindCD method is in Algorithm 2.

A. Performance Analysis

This section analyzes the performance of the *boosted* BlindCD method, mimicking the ideas in Section III-B. Due to the space limitation, we focus on the case where \mathbf{B} is sparse, *i.e.*, we select $g_1(\hat{\mathbf{B}})$ in (34) when solving (33).

Our first step towards deriving a theoretical bound for the performance of boosted BlindCD is to characterize the estimation error of $\mathcal{H}(\mathbf{S})\mathbf{B}$ when solving (29), defined as

$$\mathcal{E} := \mathcal{H}^* - \mathcal{H}(\mathbf{S})\mathbf{B}. \quad (37)$$

Lemma 2 Suppose that $L \geq R$, $\{\mathbf{z}^\ell\}_{\ell=1}^L$ spans \mathbb{R}^R , and $\|\mathbf{w}^\ell(\mathbf{z}^\ell)^\top\| < \infty$ almost surely. For every $c > 0$ and with probability at least $1 - 2c$, it holds that

$$\|\mathcal{E}\|_2 = \mathcal{O}\left(\frac{\sigma_w \log((N+R)/c)}{\sqrt{L}}\right). \quad (38)$$

The proof can be found in Appendix B. Lemma 2 captures the expected behavior of a vanishing estimation error when $L \rightarrow \infty$. Next, we show that $\hat{\mathbf{S}}^*$ from (33) is close to $\tilde{\mathcal{H}}(\mathbf{S})\mathbf{B}$ by leveraging the fact that the latter is approximately rank- K .

Lemma 3 [36, Corollary 1] Consider problem (33) with

$$\begin{aligned} \kappa &\geq 4\|\mathcal{E}\|_2, \quad \rho \geq 4\left(\frac{\alpha}{\sqrt{NR}} + \|\text{vec}(\mathcal{E})\|_\infty\right), \\ \alpha &\geq \sqrt{NR} \|\text{vec}(\tilde{\mathcal{H}}(\mathbf{S})\mathbf{B})\|_\infty. \end{aligned} \quad (39)$$

Let $R \geq K$. There exists constants c_1, c_2 such that

$$\begin{aligned} \|\hat{\mathbf{S}}^* - \tilde{\mathcal{H}}(\mathbf{S})\mathbf{B}\|_{\text{F}}^2 + \|\hat{\mathbf{B}}^* - \tilde{\mathbf{h}}_N \mathbf{B}\|_{\text{F}}^2 &\leq \\ c_1 \kappa^2 \left(K + \frac{1}{\kappa} \sum_{j=K+1}^R \sigma_j(\tilde{\mathcal{H}}(\mathbf{S})\mathbf{B}) \right) + c_2 \rho^2 \|\text{vec}(\mathbf{B})\|_0. \end{aligned} \quad (40)$$

The term $\sum_{j=K+1}^R \sigma_j(\tilde{\mathcal{H}}(\mathbf{S})\mathbf{B})$ is negligible when $\tilde{\mathcal{H}}(\mathbf{S})\mathbf{B}$ is approximately rank- K . Therefore, the implication is that the distance between $\hat{\mathbf{S}}^*$ and $\tilde{\mathcal{H}}(\mathbf{S})\mathbf{B}$ can be bounded by the sum of two terms — one that is dependent on \mathcal{E} , and one that is dependent on α/\sqrt{NR} . Overall, it shows that the error reduces when the excitation rank R and number of observations L increases. On the other hand, (39) suggest that one should set $\kappa = c_1/\sqrt{L}$, $\rho = c_2/\sqrt{RL}$ in (33) for some c_1, c_2 .

Having established these results, the boosted BlindCD method is an approximation of BlindCD operating on the boosted LPGF $\tilde{\mathcal{H}}(\mathbf{S})\mathbf{B}$. Next, we define the SVD of $\tilde{\mathcal{H}}(\mathbf{S})\mathbf{B}$ as $\tilde{\mathbf{V}} \tilde{\Sigma} \tilde{\mathbf{Q}}^\top$ and analyze the performance of the boosted BlindCD through a minor modification of Theorem 1.

Corollary 1 Suppose that Conditions 1 to 4 in Theorem 1 are met when replacing \mathbf{Q}_K by $\tilde{\mathbf{Q}}_K$ and $\mathcal{H}(\mathbf{S})$ by $\tilde{\mathcal{H}}(\mathbf{S})$. Let $\tilde{\Delta} := \hat{\mathbf{S}}^* - \tilde{\mathcal{H}}(\mathbf{S})\mathbf{B}$ and assume that

$$\tilde{\delta} := \sigma_K(\tilde{\mathcal{H}}(\mathbf{S})\mathbf{B}) - \sigma_{K+1}(\tilde{\mathcal{H}}(\mathbf{S})\mathbf{B}) - \|\tilde{\Delta}\|_2 > 0. \quad (41)$$

Then,

$$\begin{aligned} \sqrt{F(\tilde{\mathcal{C}}_1, \dots, \tilde{\mathcal{C}}_K)} - \sqrt{(1+\epsilon)F^*} &\leq \\ (2+\epsilon)\sqrt{2K} \left(\sqrt{\frac{\tilde{\gamma}^2}{1+\tilde{\gamma}^2}} + \frac{\|\tilde{\Delta}\|_2}{\tilde{\delta}} \right), \end{aligned} \quad (42)$$

where $F(\cdot)$, F^* are defined in (8), (24), respectively, and

$$\tilde{\gamma} \leq \tilde{\eta} \|\mathbf{V}_{N-K}^\top \mathbf{B} \tilde{\mathbf{Q}}_K\|_2 \|(\mathbf{V}_K^\top \mathbf{B} \tilde{\mathbf{Q}}_K)^{-1}\|_2, \quad (43)$$

where $\tilde{\eta}$ is the low-pass coefficient of the boosted LPGF $\tilde{\mathcal{H}}(\mathbf{S})\mathbf{B}$.

The proof of Corollary 1 can be found in Appendix C. We see that the performance of the boosted BlindCD method depends on $\tilde{\eta}$, the low-pass coefficient of the boosted LPGF.

While the bound in (42) is similar to that in Theorem 1, we observe that applying Lemma 2 and Lemma 3 yields

$$\|\tilde{\Delta}\|_2 \leq \|\tilde{\Delta}\|_F = \mathcal{O} \left(\sigma_{K+1}(\tilde{\mathcal{H}}(\mathbf{S})\mathbf{B}) + \frac{1}{\sqrt{L}} + \frac{1}{\sqrt{NR}} \right).$$

From the definition of $\tilde{\delta}$ we have

$$\frac{\|\tilde{\Delta}\|_2}{\tilde{\delta}} = \mathcal{O} \left(\frac{\sigma_{K+1}(\tilde{\mathcal{H}}(\mathbf{S})\mathbf{B}) + 1/\sqrt{L} + 1/\sqrt{NR}}{\sigma_K(\tilde{\mathcal{H}}(\mathbf{S})\mathbf{B}) - C\sigma_{K+1}(\tilde{\mathcal{H}}(\mathbf{S})\mathbf{B})} \right), \quad (44)$$

for some constant C . Substituting (44) into (42) shows that the sub-optimality of boosted BlindCD can be minimized when 1) the spectral gap for the sketched matrix $\tilde{\mathcal{H}}(\mathbf{S})\mathbf{B}$, 2) the number of samples L , and 3) the excitation rank R , are large. We remark that it is possible to undertake analogous performance analysis for the other proposed regularizers on \mathbf{B} [cf. (35) and (36)]. For example, this can be done using [38] and replacing Lemma 3 with the corresponding result. These extensions, however, are beyond the scope of the current paper.

V. APPLICATIONS AND NUMERICAL EXAMPLES

To illustrate the efficacy of the BlindCD methods, we study three application examples that pertain to consensus dynamics, consumer networks, and social networks. Numerical examples will be given for these applications.

Unless otherwise specified, the graphs used in the simulations will be generated according to a *stochastic block model* (SBM) [39], denoted by $G \sim \text{SBM}(N, K, a, b)$, such that G has N nodes, K equal sized communities and the intra (resp. inter) community connectivity probability is $a \in [0, 1]$ (resp. $b \in [0, 1]$). The weights on the graph, A_{ij} , are set to 1 if $(i, j) \in E$ and 0 otherwise. We use the ground truth community membership in generating the SBM graphs when evaluating the accuracies. The error rate is given by

$$P_e := \mathbb{E} \left[\frac{1}{N} \min_{\pi: [K] \rightarrow [K]} \sum_{i=1}^N \mathbb{1}_{\pi(c_i) \neq c_i^{\text{true}}} \right], \quad (45)$$

and the expectation is approximated via Monte-Carlo simulations, where $\mathbb{1}_{\mathcal{E}}$ is an indicator function for the event \mathcal{E} , $\pi : [K] \rightarrow [K]$ is a permutation function and $c_i \in [K]$ (resp. c_i^{true}) is the detected (resp. true) community membership of node i .

A. Consensus Dynamics

We first evaluate the performance of BlindCD using graph signals generated according to the observation model in (10). In particular, we focus on the consensus dynamics graph filter in Example 1. We perform Monte-Carlo simulations to evaluate the community detection performance on random graphs. In this example, the SBM graphs generated are $G \sim \text{SBM}(N, K, 8 \log N/N, \log N/N)$ with $N = 150$ and $K = 3$. We simulate a scenario where the graph filter is excited on only R nodes. In this case, the sketch matrix \mathbf{B} is generated by first picking R rows uniformly from the N available rows, and the elements in each selected rows are set to one uniformly with probability $p_b = 0.5$. For the boosted BlindCD method, we test the formulation of (33) with regularizers $g_1(\hat{\mathbf{B}})$ and $g_2(\hat{\mathbf{B}})$

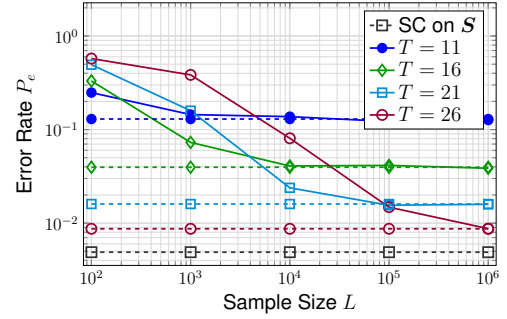


Fig. 1. **Community detection performance versus sample size L .** We consider graphs generated as $G \sim \text{SBM}(N, K, 8 \log N/N, \log N/N)$ with $N = 150, K = 3$ and fix the excitation rank at $R = 15$. The solid (resp. dashed) lines show the performance of BlindCD on the sampled output covariance \hat{C}_y (resp. true and noiseless covariance \bar{C}_y).

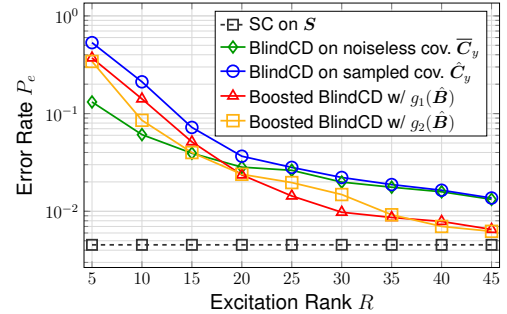


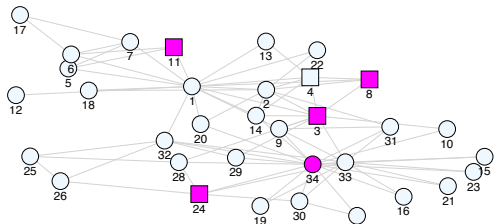
Fig. 2. **Community detection performance versus excitation rank R .** We consider graphs generated as $G \sim \text{SBM}(N, K, 8 \log N/N, \log N/N)$ with $N = 150, K = 3$ and fixed $T = 16, L = 10^3$.

[cf. (34) and (35)] by setting $\kappa = 2/\sqrt{L}$ and $\rho = 0.5/\sqrt{RL}$. The variance of observation noise is $\sigma_w^2 = 10^{-2}$ and each element of \mathbf{z}^ℓ is generated independently as $[\mathbf{z}^\ell]_i \sim \mathcal{U}[-1, 1]$.

The first example examines the effect of the graph filter's low-pass coefficient η and sample size L on the performance of BlindCD. In particular, Fig. 1 shows the performance of community detection for different filter orders T against the number of samples L accrued. Notice that the low-pass coefficient η decreases with the filter order T [cf. (18)]. As such, we observe that the performance improves with T . The error rate approaches that achieved by applying spectral clustering on the actual \mathbf{S} . An interesting observation is that for sample covariances, as T increases, the sample size L required to reach the performance of noiseless covariance also increases. This can be explained with the condition (25) in Theorem 1. In particular, as T increases, the absolute value of $\beta_K(\bar{C}_y) - \beta_{K+1}(\bar{C}_y)$ decreases, therefore restricting $\|\hat{C}_y - \bar{C}_y\|_2$ to be smaller [cf. (25)]. The latter is satisfied when the number of samples accrued is sufficiently large.

The second example shows the effect of the excitation rank R and the efficacy of the boosted BlindCD method. The results are shown in Fig. 2 where we have fixed $L = 10^3$ and $T = 16$. We observe that the performance improves with the rank R . As predicted by Corollary 1, the boosting technique enhances the performance of BlindCD.

The example in Fig. 3 shows the performance of an instance of BlindCD on the Zachary's Karate Club network when the graph signals are generated from the consensus dynamics. To capitalize on the benefit of the *boosting* technique, we consider



(a) Zachary's karate club network. Highlighted nodes in magenta are the actual sites of excitations, while nodes marked as rectangles are the detected sites of excitations using boosted BlindCD. The only mismatches were node '4' and '34'.

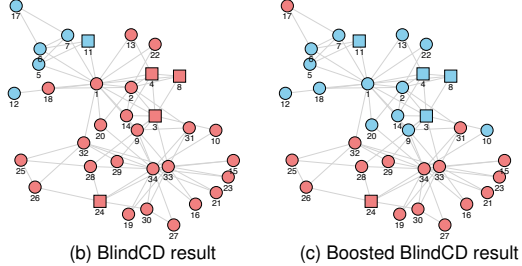


Fig. 3. **Experiments on Zachary's karate club network.** The network consists of $N = 34$ nodes and (approximately) $K = 2$ communities. The graph filter models a consensus dynamics with an order of $T = 6$ and the graph signals observed have only rank $R = 5$ as only 5 nodes are injected with input signals. The bottom plots show the result of both BlindCD methods.

a scenario with a filter order of $T = 6$, observation rank of $R = 5$ (the graph is excited on just 5 nodes) and we observe $L = 10^3$ noisy samples of the graph signals. Observe that the low-pass coefficient for the filter may be close to 1 as T is small. This explains the poorer performance of BlindCD in the subplot (b). The boosted BlindCD, instead, delivers good performance as it identifies the two communities in the network except for a miss-classification of agent 17. Through sorting the row sums of the estimated $\hat{\mathbf{B}}$, we also detected the sites of the excitations, as shown in the subplot (a).

We next describe case studies to demonstrate that the BlindCD methods can robustly detect the communities for different types of graph filters, even when the theoretical conditions are only approximately satisfied.

B. Case Studies with Network Dynamics Models

We describe applications of our BlindCD methods on detecting communities in consumer and social networks. We demonstrate how the stationary points resulting from various network dynamics models naturally fit into the formalism of LPGFs established in this paper. As we shall show later, the network dynamics in both applications can be approximated by a single-pole IIR filter [cf. Example 3].

1) *Pricing Experiments in Consumer Networks:* We apply BlindCD to detect communities in a consumer network by observing the consumers' behavior as they are subject to pricing experiments. We closely follow the model proposed in [25], [26]. The N -agent consumer network is represented as an *undirected*, weighted graph $G = (V, E, \mathbf{A})$ with $A_{ij} = A_{ji} \geq 0$ being the influence strength between agents i and j .

Consider performing L pricing experiments on the network. For $\ell \in \{1, \dots, L\}$, agent i consumes/purchases y_i units of a

product depending on (i) the price of the product p_i^ℓ and (ii) the consumption levels of the other agents who are neighbors of him/her in the network. More precisely, the consumption level y_i is determined by maximizing the utility

$$u_i(y_i, \mathbf{y}_{-i}, p_i^\ell) := ay_i - \frac{b}{2}y_i^2 + y_i \sum_{j=1}^N A_{ij}y_j - p_i^\ell y_i, \quad (46)$$

where $a, b \geq 0$ are model parameters and $\mathbf{y}_{-i} := (y_j)_{j \neq i}$. The consumption game equilibrium is

$$y_i^\ell = \arg \max_{y_i \in \mathbb{R}_+} u_i(y_i, \mathbf{y}_{-i}^\ell, p_i^\ell), \quad \forall i. \quad (47)$$

Now, under the conditions that $b > \sum_{j=1}^N A_{ij}$ and $a > p_i^\ell$, the equilibrium to the above game is unique and it satisfies

$$\mathbf{y}^\ell = (b\mathbf{I} - \mathbf{A})^{-1}(a\mathbf{1} - \mathbf{p}^\ell). \quad (48)$$

We consider the following zero-mean version of \mathbf{y}^ℓ

$$\tilde{\mathbf{y}}^\ell := \frac{1}{L} \sum_{\tau=1}^L \mathbf{y}^\tau - \mathbf{y}^\ell = (b\mathbf{I} - \mathbf{A})^{-1}\tilde{\mathbf{p}}^\ell, \quad (49)$$

where $\tilde{\mathbf{p}}^\ell := \mathbf{p}^\ell - (1/L) \sum_{\ell=1}^L \mathbf{p}^\ell$ can be interpreted as a vector of discounts to agents during the ℓ th experiment.

Our goal is to detect communities in G from the graph signals $\{\mathbf{y}^\ell\}_{\ell=1}^L$ observed from L sets of prices $\{\mathbf{p}^\ell\}_{\ell=1}^L$ imposed on the network. In fact, (49) can be interpreted as a graph filter process by recognizing $\tilde{\mathbf{p}}^\ell$ as the 'input' graph signal and $\tilde{\mathbf{y}}^\ell$ as the 'output' graph signal. In detail, since the diagonal matrix $\tilde{\mathbf{D}} := \text{Diag}(b\mathbf{1} - \mathbf{A}\mathbf{1})$ is positive definite, we can write

$$\begin{aligned} (b\mathbf{I} - \mathbf{A})^{-1} &= (\tilde{\mathbf{D}} + \mathbf{S})^{-1} \\ &= \tilde{\mathbf{D}}^{-\frac{1}{2}}(\mathbf{I} + \tilde{\mathbf{D}}^{-\frac{1}{2}}\mathbf{S}\tilde{\mathbf{D}}^{-\frac{1}{2}})^{-1}\tilde{\mathbf{D}}^{-\frac{1}{2}}. \end{aligned} \quad (50)$$

This shows that the linear operator $(b\mathbf{I} - \mathbf{A})^{-1}$ is indeed a *scaled* graph filter defined on a modified Laplacian $\tilde{\mathbf{D}}^{-\frac{1}{2}}\mathbf{S}\tilde{\mathbf{D}}^{-\frac{1}{2}}$, as we observe that $(\mathbf{I} + \tilde{\mathbf{D}}^{-\frac{1}{2}}\mathbf{S}\tilde{\mathbf{D}}^{-\frac{1}{2}})^{-1}$ is a polynomial of the modified Laplacian. For the case where $\tilde{\mathbf{D}} \approx c\mathbf{I}$, e.g., the graph is regular, the graph filter can be further approximated as

$$(b\mathbf{I} - \mathbf{A})^{-1} \approx c^{-1}(\mathbf{I} + c^{-1}\mathbf{S})^{-1} := c^{-1}\mathcal{H}_3(\mathbf{S}), \quad (51)$$

which is a single-pole IIR filter in Example 3. The observed process can thus be attributed to that of an LPGF.

Next, let us study the types of the 'input' signals involved. A practical case is when the pricing experiments only control the prices on R agents, while keeping the prices of the rest unchanged across experiments. This gives rise to a low-rank structure for the input signal. Note that $\tilde{\mathbf{p}}^\ell = \mathbf{B}\mathbf{z}^\ell$ holds with

$$[\mathbf{B}]_{\mathcal{I},:} = \mathbf{I}, [\mathbf{B}]_{[N] \setminus \mathcal{I},:} = \mathbf{0}, \quad (52)$$

where $\mathcal{I} \subset [N]$ is the index set of R agents whom prices are controlled, and $\mathbf{z}^\ell \in \mathbb{R}^R$ is simply a vector of the price variations from the mean. We observe that

$$\tilde{\mathbf{y}}^\ell \approx c^{-1}\mathcal{H}_3(\mathbf{S})\mathbf{B}\mathbf{z}^\ell. \quad (53)$$

Note that our model is similar to [26], yet [26] assumes that the pricing experiments control prices on *all* agents.

One may apply the *boosted* BlindCD method to the community detection problem. As the sketching matrix \mathbf{B} is sparse for this example, we see that (33) with $g(\hat{\mathbf{B}}) = \|\text{vec}(\hat{\mathbf{B}})\|_1$ can be applied directly.

2) *Opinion Dynamics in Social Networks*: This case study applies BlindCD to detect communities in a social network from opinion dynamics. We focus on a social network with N agents, which is represented by a *directed* graph $G = (V, E, \mathbf{A})$ such that $A_{ij} \geq 0$ captures the amount of ‘trust’ that agent i has on agent j . The agents are influenced by R external agents who are *stubborn* such that their opinions are not influenced by the others [40]–[42].

Consider L discussions in the social network on various topics. During the ℓ th discussion, the agents exchange opinions according to the DeGroot opinion dynamics with stubborn agents [27] — let $y_i^\ell(\tau)$ (*resp.* z_j^ℓ) be the opinion of the i th agent (*resp.* j th stubborn agent) at time τ , e.g., $y_i^\ell(\tau) \in [0, 1]$ represents the probability for agent i to agree on the ℓ th topic, we have

$$\mathbf{y}^\ell(\tau + 1) = \mathbf{A}\mathbf{y}^\ell(\tau) + \mathbf{B}\mathbf{z}^\ell, \quad \tau = 1, 2, \dots, \quad (54)$$

where $\mathbf{B} \in \mathbb{R}^{N \times R}$ is a weighted adjacency matrix describing the bipartite graph that connects the stubborn agents to the agents in G . We assume that the concatenated matrix is stochastic such that $[\mathbf{A}, \mathbf{B}]\mathbf{1} = \mathbf{1}$ and therefore the updated opinions are convex combinations of the opinions of neighboring agents; see [22] for detailed description on the model.

Let us focus on the *steady-state* opinions, *i.e.*, the opinions when $\tau \rightarrow \infty$. Under mild assumptions, it holds [22], [43]

$$\begin{aligned} \mathbf{y}^\ell &:= \lim_{\tau \rightarrow \infty} \mathbf{y}^\ell(\tau) = (\mathbf{I} - \mathbf{A})^{-1} \mathbf{B} \mathbf{z}^\ell \\ &= (\text{Diag}(\mathbf{1} - \mathbf{A}\mathbf{1}) + \mathbf{S})^{-1} \mathbf{B} \mathbf{z}^\ell \\ &\approx c^{-1} (\mathbf{I} + c^{-1} \mathbf{S})^{-1} \mathbf{B} \mathbf{z}^\ell = c^{-1} \mathcal{H}_3(\mathbf{S}) \mathbf{B} \mathbf{z}^\ell, \end{aligned} \quad (55)$$

where the last approximation holds when there exists $c > 0$ such that $c\mathbf{1} \approx \mathbf{1} - \mathbf{A}\mathbf{1} = \mathbf{B}\mathbf{1}$, e.g., when the out-degrees of the stubborn agents are almost the same.

Our aim is detecting communities in G using the graph signals $\{\mathbf{y}^\ell\}_{\ell=1}^L$ and the initial opinions $\{\mathbf{z}^\ell\}_{\ell=1}^L$. The observation in (55) is akin to that presented for consumer networks [cf. (48)]. Despite the similarity to the previous examples, it is important to note that the Laplacian matrix \mathbf{S} can be asymmetric. As a simplifying assumption we can assume that \mathbf{S} is approximately symmetric and anticipate that BlindCD would work in this case. This symmetry in \mathbf{S} is consistent with assuming that trust in social networks is of mutual nature².

3) *Numerical Examples*: We generate graphs G as $G \sim \text{SBM}(150, 3, 8 \log N/N, \log N/(2N))$, $N = 150$. For the *consumer* networks, \mathbf{A} is taken as the binary adjacency matrix of G and \mathbf{B} is chosen as in (52) where the set of affected agents \mathcal{I} is selected uniformly. Furthermore, in the utility (46), we set $b = 2\|\mathbf{A}\mathbf{1}\|_\infty$ and $a = 2 \max_\ell \|\mathbf{p}^\ell\|_\infty$ such that the equilibrium always satisfies (48). For the *social* networks, we first generate the support of \mathbf{B} as a sparse bipartite graph with connectivity $2 \log N/N$, then the weights on \mathbf{A}, \mathbf{B} are assigned uniformly such that all the rows in the concatenated

²Additional numerical experiments show that, on a directed graph where the trusts are not mutual, the BlindCD method recovers the same sets of nodes that are discovered by performing K -means on the top *eigenvectors* of the adjacency matrix \mathbf{A} . We omit these interesting results here since their interpretation requires a different notion of community for directed graphs, e.g., see [44]. Further investigations on this subject are left for future work.

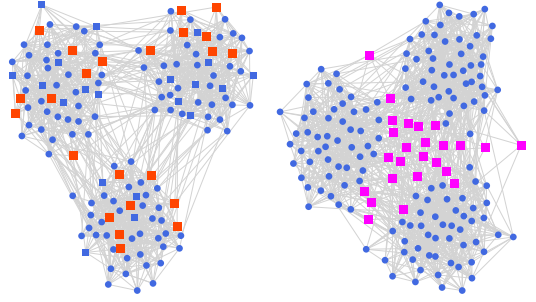


Fig. 4. **Snapshots of set-ups for case studies on network dynamics.** (Left) A consumers network, where the highlighted nodes are the agents that the pricing experiments were performed on. (Right) A social network, where the highlighted nodes are the stubborn agents. Both networks are generated according to $\text{SBM}(150, 3, 8 \log N/N, \log N/(2N))$.

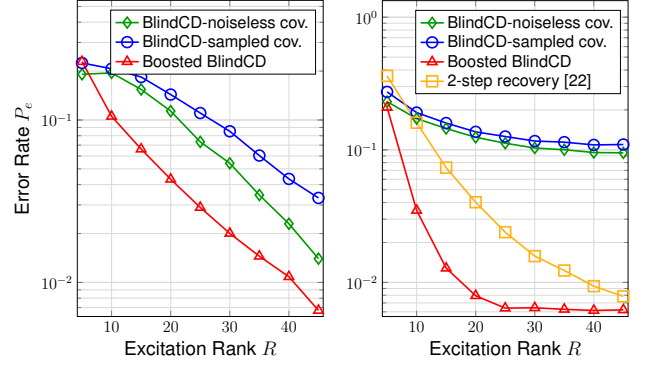
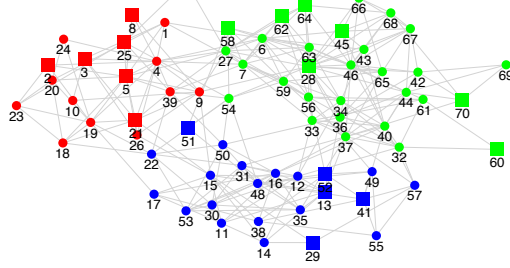


Fig. 5. **Community detection performance on cases of network dynamics.** (Left) Pricing experiments on consumers network. (Right) Opinion dynamics with stubborn agents on social networks. In both cases, we consider networks generated as $G \sim \text{SBM}(N, 3, 8 \log N/N, \log N/(2N))$, $N = 150$.

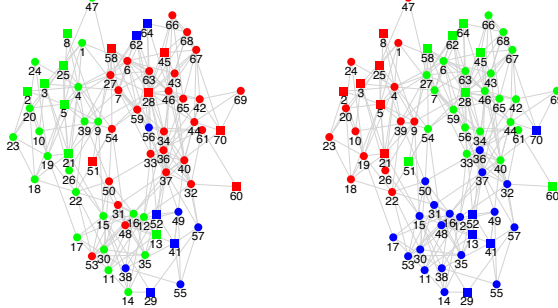
matrix $[\mathbf{A}, \mathbf{B}]$ sum up to one. This models a setting where the stubborn agents are connected sparsely to the others, *i.e.*, they are located at the *periphery of the communities*. Note the support of \mathbf{A} is symmetric with $A_{ij} \neq 0 \Leftrightarrow A_{ji} \neq 0$. Snapshots of the set-ups for both networks are found in Fig. 4.

The consumption levels and steady-state opinions can both be approximated as processes generated from a single-pole IIR graph filter as in Example 3. The difference between the two cases rests on the design of the sketch matrix \mathbf{B} . In the following, we fix the number of samples at $L = 10^4$ with a noise variance of $\sigma_w^2 = (10^{-1}/b^2)^2$ for consumer networks and $\sigma_w^2 = 10^{-2}$ for social networks. For the boosted BlindCD method, we set $\kappa = 2/\sqrt{L}, \rho = 4/\sqrt{RL}$ for consumer networks and $\kappa = 2/\sqrt{L}, \rho = 1/\sqrt{RL}$ for social networks; and we test the formulation of (33) with the regularizer $g_1(\hat{\mathbf{B}})$. For the social network, we included a comparison to the parametric method in [22] which involves first recovering the complete graph topology, and then applying spectral clustering on the inferred topology.

The results of our numerical experiments are shown in Fig. 5, where we compare the community detection performance as the excitation rank R increases in both systems. Similar to the previous experiment in Fig. 2, for both cases we observe that the performance improves with R and the boosted BlindCD method delivers the best performance consistently. Overall, the performance improvement with boosted BlindCD is greater than in the previous example [cf. Fig. 2]. The reason behind this is the fact that the IIR graph filter has a poor low-



(a) **Highschool** network. The pricing experiments modify prices for the agents marked with *square*. The above clustering on the network is computed from the true Laplacian matrix S , which has a RatioCut of 3.618.

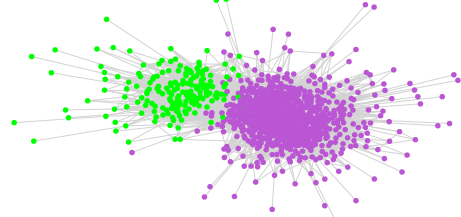


(b) BlindCD, RatioCut= 6.769. (c) Boosted BlindCD, RatioCut= 4.701.

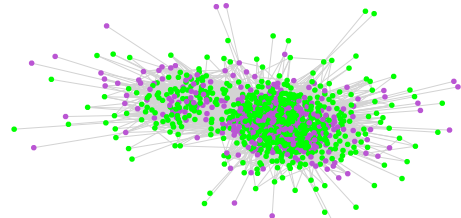
Fig. 6. **Pricing experiments on the Highschool network.** The network comprises of $N = 70$ agents and (approximately) $K = 3$ communities. The utility parameters in (46) are $a = R$ and $b = 2\|A1\|_\infty$. The network's equilibrium consumption levels are collected for $L = 10^3$ samples, each observed with a noise variance of $\sigma_w^2 = 10^{-2}/b^4$. The pricing experiments are conducted through controlling the prices for $R = 18$ agents.

pass coefficient depending on the parameter $c \gg 1$ for the scenario we have considered. Another observation is that the community detection performance of the un-boosted BlindCD saturates at $R \approx 25$ for the opinion dynamics experiments while it continues to improve with R for pricing ones. This is due to the different model used for the sketch matrix \mathbf{B} . In particular, for the pricing experiments, \mathbf{B} is merely a sub-matrix of the identity matrix. Recall from Theorem 1 that the performance of BlindCD depend on the product $\|\mathbf{V}_{N-K}^\top \mathbf{B} \mathbf{Q}_K\|_2 \|\mathbf{V}_K^\top \mathbf{B} \mathbf{Q}_K\|^{-1}\|_2$, which is anticipated to decrease since \mathbf{B} approaches a permutation of \mathbf{I} as R approaches N , yielding a better performance. However, the same observation does not apply for opinion dynamics as the sketch matrix does not approximate the identity matrix as R grows.

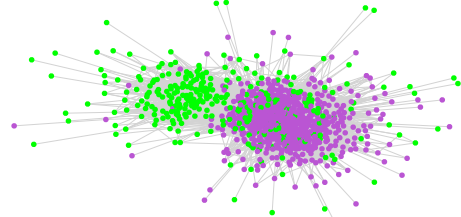
We conclude the section by illustrating an application on real network topologies for the two network dynamics. Fig. 6 shows an example of simulated pricing experiments on the network `highschool` from [45], which is a friendship network between $N = 70$ high school students with $|E| = 273$ undirected edges. On the other hand, Fig. 7 shows the case study for opinion dynamics on the Facebook network of `ReedCollege` [46], which is a friendship network with $N = 962$ college students with $|E| = 18,812$ undirected edges, and we influence the network using $R = 150$ stubborn agents. To handle the high dimensionality, we applied the fast algorithm from [47] to solve the robust PCA problem in (33). In both cases, we observe that the boosted BlindCD method



(a) **ReedCollege** network. The clustering above is found by applying spectral clustering on the true S . The obtained RatioCut is 0.1419 w.r.t. A .



(b) Applying BlindCD method. The obtained RatioCut is 0.8953 w.r.t. A .



(c) Applying Boosted BlindCD method. The obtained RatioCut is 0.5249 w.r.t. A .

Fig. 7. **Opinion dynamics experiments on ReedCollege network.** The network comprises of $N = 962$ agents and (approximately) $K = 2$ communities. The network's steady-state opinions are collected with $L = 10^4$ samples, each observed with a noise variance of $\sigma_w^2 = 10^{-2}$. There are $R = 150$ stubborn agents in the experiments, which are connected to the social network through a random bi-partite graph with connectivity $\log N/N$.

recovers the communities in the networks, as evidenced from the illustrations and the ratio-cut score obtained.

VI. CONCLUSIONS

This paper proposes a set of *blind* community detection methods for inferring community structure from graph signals. Instead of relying on a full-rank excitation model, we consider a challenging and realistic setting where the graph signals are outputs of a graph filter with low-rank excitations. The BlindCD methods rely on an intrinsic *low-pass* property of the graph filters that models the network dynamics. This property holds for common network processes and the accuracy of BlindCD is analyzed by viewing the graph signals as sketches of the graph filters. We propose a boosting technique to improve the performance of BlindCD. The technique leverages the latent ‘low-rank plus sparse’ structure related to the graph signals. Extensive numerical experiments verify our findings.

APPENDIX A PROOF OF THEOREM 1

To simplify the notations while proving the theorem, let us define the following indicator matrices for the communities. Firstly, the matrix $\hat{\mathbf{X}} \in \mathbb{R}^{N \times K}$ is associated with the communities $\{\hat{\mathcal{C}}_1, \dots, \hat{\mathcal{C}}_K\}$ found with BlindCD and is defined as

$$\hat{X}_{ij} := \begin{cases} 1/\sqrt{|\hat{\mathcal{C}}_j|}, & \text{if } i \in \hat{\mathcal{C}}_j \\ 0, & \text{otherwise.} \end{cases} \quad (56)$$

Recall that $\widehat{\mathbf{V}}_K$ represents the projector onto the principal K -dimensional subspace of $\widehat{\mathbf{C}}_y$ (see Algorithm 1). We have

$$\|\widehat{\mathbf{V}}_K - \widehat{\mathbf{X}}\widehat{\mathbf{X}}^\top\widehat{\mathbf{V}}_K\|_F^2 = \sum_{k=1}^K \sum_{i \in \mathcal{C}_k} \left\| \widehat{\mathbf{v}}_i^{\text{row}} - \frac{1}{|\mathcal{C}_k|} \sum_{j \in \mathcal{C}_k} \widehat{\mathbf{v}}_j^{\text{row}} \right\|_2^2.$$

Define \mathcal{X} as the set of all possible indicator matrices of partitions. Using Condition 1 in Theorem 1, we have that

$$\begin{aligned} \|\widehat{\mathbf{V}}_K - \widehat{\mathbf{X}}\widehat{\mathbf{X}}^\top\widehat{\mathbf{V}}_K\|_F^2 &\leq (1+\epsilon) \min_{\mathbf{X} \in \mathcal{X}} \|\widehat{\mathbf{V}}_K - \mathbf{X}\mathbf{X}^\top\widehat{\mathbf{V}}_K\|_F^2 \\ &\leq (1+\epsilon) \|\widehat{\mathbf{V}}_K - \mathbf{X}^*(\mathbf{X}^*)^\top\widehat{\mathbf{V}}_K\|_F^2, \end{aligned} \quad (57)$$

where we have defined $\mathbf{X}^* \in \mathbb{R}^{N \times K}$ by replacing \mathcal{C}_i in (56) with \mathcal{C}_i^* such that $\mathcal{C}_1^*, \dots, \mathcal{C}_K^*$ is an optimal set of communities found by minimizing $F(\mathcal{C}_1, \dots, \mathcal{C}_K)$ [cf. (8)]. On the other hand, by the definition,

$$\begin{aligned} \|\mathbf{V}_K - \mathbf{X}^*(\mathbf{X}^*)^\top\mathbf{V}_K\|_F^2 &= \min_{\mathbf{X} \in \mathcal{X}} \|\mathbf{V}_K - \mathbf{X}\mathbf{X}^\top\mathbf{V}_K\|_F^2 \\ &= \min_{\mathcal{C}_1, \dots, \mathcal{C}_K} F(\mathcal{C}_1, \dots, \mathcal{C}_K) = F^*, \end{aligned} \quad (58)$$

and furthermore $\|\mathbf{V}_K - \widehat{\mathbf{X}}\widehat{\mathbf{X}}^\top\mathbf{V}_K\|_F^2 = F(\widehat{\mathcal{C}}_1, \dots, \widehat{\mathcal{C}}_K)$.

Define the error matrix as $\mathbf{E} := \mathbf{V}_K\mathbf{V}_K^\top - \widehat{\mathbf{V}}_K\widehat{\mathbf{V}}_K^\top$. We observe the following chain of inequalities:

$$\begin{aligned} \|\mathbf{V}_K - \widehat{\mathbf{X}}\widehat{\mathbf{X}}^\top\mathbf{V}_K\|_F &= \|(\mathbf{I} - \widehat{\mathbf{X}}\widehat{\mathbf{X}}^\top)(\widehat{\mathbf{V}}_K\widehat{\mathbf{V}}_K^\top + \mathbf{E})\|_F \\ &\leq \|(\mathbf{I} - \widehat{\mathbf{X}}\widehat{\mathbf{X}}^\top)\widehat{\mathbf{V}}_K\widehat{\mathbf{V}}_K^\top\|_F + \|(\mathbf{I} - \widehat{\mathbf{X}}\widehat{\mathbf{X}}^\top)\mathbf{E}\|_F \\ &\leq \|(\mathbf{I} - \widehat{\mathbf{X}}\widehat{\mathbf{X}}^\top)\widehat{\mathbf{V}}_K\widehat{\mathbf{V}}_K^\top\|_F + \|\mathbf{E}\|_F, \end{aligned} \quad (59)$$

where the last inequality is due to the fact that $(\mathbf{I} - \widehat{\mathbf{X}}\widehat{\mathbf{X}}^\top)$ is a projection matrix. Using (57), we have that

$$\begin{aligned} &\|(\mathbf{I} - \widehat{\mathbf{X}}\widehat{\mathbf{X}}^\top)\widehat{\mathbf{V}}_K\widehat{\mathbf{V}}_K^\top\|_F + \|\mathbf{E}\|_F \\ &\leq \sqrt{1+\epsilon} \|(\mathbf{I} - \mathbf{X}^*(\mathbf{X}^*)^\top)(\mathbf{V}_K\mathbf{V}_K^\top - \mathbf{E})\|_F + \|\mathbf{E}\|_F \\ &\leq \sqrt{1+\epsilon} \|(\mathbf{I} - \mathbf{X}^*(\mathbf{X}^*)^\top)\mathbf{V}_K\mathbf{V}_K^\top\|_F \\ &\quad + \sqrt{1+\epsilon} \|(\mathbf{I} - \mathbf{X}^*(\mathbf{X}^*)^\top)\mathbf{E}\|_F + \|\mathbf{E}\|_F \\ &\leq \sqrt{1+\epsilon} \|(\mathbf{I} - \mathbf{X}^*(\mathbf{X}^*)^\top)\mathbf{V}_K\mathbf{V}_K^\top\|_F + (2+\epsilon)\|\mathbf{E}\|_F \\ &= \sqrt{(1+\epsilon)F^*} + (2+\epsilon)\|\mathbf{E}\|_F, \end{aligned} \quad (60)$$

where we have used the fact $(\mathbf{I} - \mathbf{X}^*(\mathbf{X}^*)^\top)$ is a projection matrix and $\sqrt{1+\epsilon} \leq 1+\epsilon$ in the third inequality. The final step is to bound $\|\mathbf{E}\|_F$, where we rely on the following results.

Lemma 4 [34, Lemma 7] For any $\mathbf{A}, \mathbf{B} \in \mathbb{R}^{N \times K}$ with $N \geq K$ and $\mathbf{A}^\top\mathbf{A} = \mathbf{B}^\top\mathbf{B} = \mathbf{I}$, it holds that

$$\|\mathbf{A}\mathbf{A}^\top - \mathbf{B}\mathbf{B}^\top\|_F^2 \leq 2K\|\mathbf{A}\mathbf{A}^\top - \mathbf{B}\mathbf{B}^\top\|_2^2. \quad (61)$$

Proposition 1 Under Conditions 2 to 4 in Theorem 1, we have

$$\|\overline{\mathbf{V}}_K\overline{\mathbf{V}}_K^\top - \mathbf{V}_K\mathbf{V}_K^\top\|_2^2 = (1+\gamma^2)^{-1}\gamma^2, \quad (62)$$

where the columns of $\overline{\mathbf{V}}_K$ are the top K eigenvectors of $\overline{\mathbf{C}}_y$ and γ is bounded as stated in (27).

Proposition 2 Under Condition 5 in Theorem 1, it holds that

$$\|\overline{\mathbf{V}}_K\overline{\mathbf{V}}_K^\top - \widehat{\mathbf{V}}_K\widehat{\mathbf{V}}_K^\top\|_2 \leq \|\widehat{\mathbf{C}}_y - \overline{\mathbf{C}}_y\|_2/\delta. \quad (63)$$

The proofs of the propositions can be found in the subsections A and B of this appendix. Applying Lemma 4 we obtain that

$$\|\mathbf{E}\|_F \leq \sqrt{2K}\|\mathbf{V}_K\mathbf{V}_K^\top - \widehat{\mathbf{V}}_K\widehat{\mathbf{V}}_K^\top\|_2. \quad (64)$$

Combining (62), (63) and using the triangle inequality yields

$$\begin{aligned} \sqrt{F(\widehat{\mathcal{C}}_1, \dots, \widehat{\mathcal{C}}_K)} &= \|(\mathbf{I} - \widehat{\mathbf{X}}\widehat{\mathbf{X}}^\top)\mathbf{V}_K\mathbf{V}_K^\top\|_F \\ &\leq \sqrt{(1+\epsilon)F^*} + (2+\epsilon)\sqrt{2K} \left(\sqrt{\frac{\gamma^2}{1+\gamma^2}} + \frac{\|\widehat{\mathbf{C}}_y - \overline{\mathbf{C}}_y\|_2}{\delta} \right), \end{aligned}$$

concluding the proof.

A. Proof of Proposition 1

We begin our proof by establishing the relationships between $\overline{\mathbf{V}}_K, \mathbf{V}_K$ and the left singular vectors of $\mathcal{H}(\mathbf{S})\mathbf{B}$. Denote the rank- K approximation to $\mathcal{H}(\mathbf{S})$ as $[\mathcal{H}(\mathbf{S})]_K := \mathbf{V}_K \text{diag}(\tilde{\mathbf{h}}_K) \mathbf{V}_K^\top$. This expression is valid due to the low pass property of $\mathcal{H}(\mathbf{S})$. Define $\tilde{\mathbf{B}} := \mathbf{B}\mathbf{Q}_K$, we observe that

$$\mathcal{R}([\mathcal{H}(\mathbf{S})]_K) = \mathcal{R}([\mathcal{H}(\mathbf{S})]_K \tilde{\mathbf{B}}), \quad (65)$$

which is due to Condition 3 in Theorem 1 such that the linear transformation $\tilde{\mathbf{B}}$ does not modify the range space of $[\mathcal{H}(\mathbf{S})]_K$. Similarly, $[\overline{\mathbf{C}}_y]_K := \overline{\mathbf{V}}_K \text{diag}(\boldsymbol{\sigma}_K)^2 \overline{\mathbf{V}}_K^\top$ is the rank K approximation to $\overline{\mathbf{C}}_y$. We observe the equivalences

$$\mathcal{R}([\overline{\mathbf{C}}_y]_K) = \mathcal{R}([\mathcal{H}(\mathbf{S})\mathbf{B}]_K) = \mathcal{R}(\mathcal{H}(\mathbf{S})\tilde{\mathbf{B}}) \quad (66)$$

where the last equality is due to $\mathcal{H}(\mathbf{S})\tilde{\mathbf{B}} = \mathcal{H}(\mathbf{S})\mathbf{B}\mathbf{Q}_K = \overline{\mathbf{V}}_K \text{diag}(\boldsymbol{\sigma}_K)$, as we recall that the columns of \mathbf{Q}_K are the top K right singular vectors of $\mathcal{H}(\mathbf{S})\mathbf{B}$. Furthermore,

$$\mathcal{R}([\mathcal{H}(\mathbf{S})]_K \tilde{\mathbf{B}}) \perp \mathcal{R}((\mathcal{H}(\mathbf{S}) - [\mathcal{H}(\mathbf{S})]_K)\tilde{\mathbf{B}}). \quad (67)$$

Let the columns of $\tilde{\mathbf{V}}_K$ and $\tilde{\overline{\mathbf{V}}}_K$ be respectively the top- K singular vectors of $[\mathcal{H}(\mathbf{S})]_K \tilde{\mathbf{B}}$ and $\mathcal{H}(\mathbf{S})\tilde{\mathbf{B}}$, therefore (65) and (66) imply that $\mathbf{V}_K\mathbf{V}_K^\top = \tilde{\mathbf{V}}_K\tilde{\mathbf{V}}_K^\top$ and $\overline{\mathbf{V}}_K\overline{\mathbf{V}}_K^\top = \tilde{\overline{\mathbf{V}}}_K\tilde{\overline{\mathbf{V}}}_K^\top$. Invoking (67) with [48, Lemma 8] through setting $\mathbf{D} = \mathcal{H}(\mathbf{S})\tilde{\mathbf{B}}$, $\mathbf{C} = [\mathcal{H}(\mathbf{S})]_K \tilde{\mathbf{B}}$ and $\mathbf{E} = (\mathcal{H}(\mathbf{S}) - [\mathcal{H}(\mathbf{S})]_K)\tilde{\mathbf{B}}$ therein, and applying [49, Theorem 2.6.1], we obtain that

$$\begin{aligned} \|\mathbf{V}_K\mathbf{V}_K^\top - \overline{\mathbf{V}}_K\overline{\mathbf{V}}_K^\top\|_2^2 &= \|\tilde{\mathbf{V}}_K\tilde{\mathbf{V}}_K^\top - \tilde{\overline{\mathbf{V}}}_K\tilde{\overline{\mathbf{V}}}_K^\top\|_2^2 \\ &= 1 - \beta_K([\mathcal{H}(\mathbf{S})]_K \tilde{\mathbf{B}} \boldsymbol{\Pi}^\dagger([\mathcal{H}(\mathbf{S})]_K \tilde{\mathbf{B}})^\top), \end{aligned} \quad (68)$$

where we have defined $\boldsymbol{\Pi} := (\mathcal{H}(\mathbf{S})\tilde{\mathbf{B}})^\top \mathcal{H}(\mathbf{S})\tilde{\mathbf{B}}$ and $\beta_K(\cdot)$ denotes the K th largest eigenvalue. Under Condition 4 in Theorem 1, the $K \times K$ matrix $\boldsymbol{\Pi}$ is non-singular. We observe the following chain of equalities

$$\begin{aligned} &\beta_K([\mathcal{H}(\mathbf{S})]_K \tilde{\mathbf{B}} \boldsymbol{\Pi}^{-1}([\mathcal{H}(\mathbf{S})]_K \tilde{\mathbf{B}})^\top) \\ &= \beta_K\left(\text{diag}(\tilde{\mathbf{h}}_K)\mathbf{V}_K^\top \tilde{\mathbf{B}} \boldsymbol{\Pi}^{-1}(\text{diag}(\tilde{\mathbf{h}}_K)\mathbf{V}_K^\top \tilde{\mathbf{B}})^\top\right) \\ &= \frac{1}{\beta_K\left((\text{diag}(\tilde{\mathbf{h}}_K)\mathbf{V}_K^\top \tilde{\mathbf{B}})^{-\top} \boldsymbol{\Pi} (\text{diag}(\tilde{\mathbf{h}}_K)\mathbf{V}_K^\top \tilde{\mathbf{B}})^{-1}\right)}, \end{aligned} \quad (69)$$

where the first equality is due to $\beta_K(\mathbf{U}\mathbf{A}\mathbf{U}^\top) = \beta_K(\mathbf{A})$ for any symmetric \mathbf{A} and $\mathbf{U} \in \mathbb{R}^{N \times K}$ with orthogonal columns, and the second equality follows since the argument in $\beta_K(\cdot)$ is of rank K . Moreover, $\boldsymbol{\Pi}$ admits the decomposition

$$\begin{aligned} \boldsymbol{\Pi} &= (\mathcal{H}(\mathbf{S})\tilde{\mathbf{B}})^\top \mathcal{H}(\mathbf{S})\tilde{\mathbf{B}} = \tilde{\mathbf{B}}^\top \mathcal{H}(\mathbf{S})^\top \mathcal{H}(\mathbf{S})\tilde{\mathbf{B}} \\ &= \tilde{\mathbf{B}}^\top \mathbf{V}_K \text{diag}(\tilde{\mathbf{h}}_K)^2 \mathbf{V}_K^\top \tilde{\mathbf{B}} \\ &\quad + \tilde{\mathbf{B}}^\top \mathbf{V}_{N-K} \text{diag}(\tilde{\mathbf{h}}_{N-K})^2 \mathbf{V}_{N-K}^\top \tilde{\mathbf{B}}. \end{aligned} \quad (70)$$

Thus, yielding that

$$\begin{aligned}
& \beta_K \left([\mathcal{H}(\mathbf{S})]_K \tilde{\mathbf{B}} \mathbf{\Pi}^{-1} ([\mathcal{H}(\mathbf{S})]_K \tilde{\mathbf{B}})^\top \right) \\
&= \left(1 + \beta_1 \left((\text{diag}(\tilde{\mathbf{h}}_K) \mathbf{V}_K^\top \tilde{\mathbf{B}})^{-\top} \tilde{\mathbf{B}}^\top \mathbf{V}_{N-K} \right. \right. \\
&\quad \left. \left. \text{diag}(\tilde{\mathbf{h}}_{N-K})^2 \mathbf{V}_{N-K}^\top \tilde{\mathbf{B}} (\text{diag}(\tilde{\mathbf{h}}_K) \mathbf{V}_K^\top \tilde{\mathbf{B}})^{-1} \right) \right)^{-1} \\
&= \frac{1}{1 + \|\text{diag}(\tilde{\mathbf{h}}_{N-K}) \mathbf{V}_{N-K}^\top \tilde{\mathbf{B}} (\text{diag}(\tilde{\mathbf{h}}_K) \mathbf{V}_K^\top \tilde{\mathbf{B}})^{-1}\|_2^2} \\
&= \left(1 + \gamma^2 \right)^{-1},
\end{aligned}$$

where we have defined γ such that

$$\begin{aligned}
\gamma &:= \|\text{diag}(\tilde{\mathbf{h}}_{N-K}) \mathbf{V}_{N-K}^\top \tilde{\mathbf{B}} (\text{diag}(\tilde{\mathbf{h}}_K) \mathbf{V}_K^\top \tilde{\mathbf{B}})^{-1}\|_2 \\
&\leq \eta \|\mathbf{V}_{N-K}^\top \mathbf{B} \mathbf{Q}_K\|_2 \|\mathbf{V}_K^\top \mathbf{B} \mathbf{Q}_K\|_2^{-1}.
\end{aligned} \tag{71}$$

Substituting the above into (68) concludes the proof.

B. Proof of Proposition 2

Denote the SVD of the sampled covariance as $\hat{\mathbf{C}}_y = \hat{\mathbf{V}} \hat{\Sigma} \hat{\mathbf{V}}^\top$. The left hand side of (63) can be written as

$$\|\bar{\mathbf{V}}_K \bar{\mathbf{V}}_K^\top - \hat{\mathbf{V}}_K \hat{\mathbf{V}}_K^\top\|_2 = \|\hat{\mathbf{V}}_{N-K}^\top \bar{\mathbf{V}}_K\|_2, \tag{72}$$

where the equality is due to [49, Theorem 2.6.1].

Define $\Delta := \hat{\mathbf{C}}_y - \bar{\mathbf{C}}_y$. Condition 5 in Theorem 1 implies that the largest eigenvalue in $\hat{\Sigma}_{N-K}$ will never exceed $\beta_K(\bar{\mathbf{C}}_y) - \delta$ since

$$\begin{aligned}
\beta_{\max}(\hat{\Sigma}_{N-K}) &= \beta_{K+1}(\hat{\mathbf{C}}_y) \leq \beta_{K+1}(\bar{\mathbf{C}}_y) + \beta_1(\Delta) \\
&\leq \beta_{K+1}(\bar{\mathbf{C}}_y) + \|\Delta\|_2,
\end{aligned} \tag{73}$$

where the first inequality is due to Weyl's inequality [49]. The perturbed matrix $\hat{\mathbf{C}}_y$ thus satisfies the requirement of the Davis-Kahan's $\sin(\Theta)$ theorem [50]

$$\|\hat{\mathbf{V}}_{N-K}^\top \bar{\mathbf{V}}_K\|_2 \leq \delta^{-1} \|\hat{\mathbf{V}}_{N-K}^\top \Delta \bar{\mathbf{V}}_K\|_2. \tag{74}$$

The inequality in (63) is obtained by observing that both $\bar{\mathbf{V}}_K$ and $\hat{\mathbf{V}}_{N-K}$ are orthogonal matrices.

APPENDIX B PROOF OF LEMMA 2

Fix $1 \geq c > 0$. Under the conditions stated in the lemma, the least-squares optimization (29) admits a closed form solution

$$\mathcal{H}^* - \mathcal{H}(\mathbf{S})\mathbf{B} = \left(\sum_{\ell=1}^L \mathbf{w}^\ell(\mathbf{z}^\ell)^\top \right) \left(\sum_{\ell=1}^L \mathbf{z}^\ell(\mathbf{z}^\ell)^\top \right)^{-1}, \tag{75}$$

where \mathbf{w}^ℓ was introduced in (10). Denoting the right hand side in (75) by \mathcal{E} , we have that

$$\begin{aligned}
\|\mathcal{E}\|_2 &= \left\| \left(\sum_{\ell=1}^L \mathbf{w}^\ell(\mathbf{z}^\ell)^\top \right) \left(\sum_{\ell=1}^L \mathbf{z}^\ell(\mathbf{z}^\ell)^\top \right)^{-1} \right\|_2 \\
&\leq \left\| \sum_{\ell=1}^L \mathbf{w}^\ell(\mathbf{z}^\ell)^\top \right\|_2 \left\| \left(\sum_{\ell=1}^L \mathbf{z}^\ell(\mathbf{z}^\ell)^\top \right)^{-1} \right\|_2.
\end{aligned} \tag{76}$$

Observe that $\frac{1}{L} \sum_{\ell=1}^L \mathbf{z}^\ell(\mathbf{z}^\ell)^\top$ converges to \mathbf{I} such that with probability at least $1 - c$,

$$\left\| \frac{1}{L} \sum_{\ell=1}^L \mathbf{z}^\ell(\mathbf{z}^\ell)^\top - \mathbf{I} \right\|_2 \leq C_0 \sqrt{\frac{R \log(1/c)}{L}}, \tag{77}$$

for some constant C_0 . Applying [51, Proposition 2.1] we get that

$$\begin{aligned}
\left\| \left(\frac{1}{L} \sum_{\ell=1}^L \mathbf{z}^\ell(\mathbf{z}^\ell)^\top \right)^{-1} \right\|_2 &\leq \left(1 - \left\| \frac{1}{L} \sum_{\ell=1}^L \mathbf{z}^\ell(\mathbf{z}^\ell)^\top - \mathbf{I} \right\|_2 \right)^{-1} \\
&\leq \left(1 - C_0 \sqrt{\frac{R \log(1/c)}{L}} \right)^{-1}.
\end{aligned}$$

On the other hand, observe that $\mathbb{E}[\mathbf{w}^\ell(\mathbf{z}^\ell)^\top] = 0$ and $\|\mathbf{w}^\ell(\mathbf{z}^\ell)^\top\| \leq C_w$ almost surely. Applying the matrix Bernstein's inequality [52, Theorem 1.6] it follows that with probability at least $1 - c$ and for sufficiently large L ,

$$\left\| \frac{1}{L} \sum_{\ell=1}^L \mathbf{w}^\ell(\mathbf{z}^\ell)^\top \right\|_2 \leq C_1 \sqrt{\frac{\sigma_w^2 \log((N+R)/c)}{L}}, \tag{78}$$

for some constant C_1 . Finally, with probability at least $1 - 2c$,

$$\|\mathcal{E}\|_2 \leq \frac{C_1 \sqrt{\sigma_w^2 \log((N+R)/c)}}{\sqrt{L} - C_0 \sqrt{R \log(1/c)}} = \mathcal{O}(\sigma_w / \sqrt{L}). \tag{79}$$

APPENDIX C PROOF OF COROLLARY 1

Recall that $\tilde{\mathbf{V}}_K$ and $\tilde{\mathbf{S}}_K$ are the top K left singular vectors of $\tilde{\mathcal{H}}(\mathbf{S})\mathbf{B}$ and $\tilde{\mathbf{S}}^*$, respectively. We can repeat the proof for Theorem 1 up to (60) by re-defining the error matrix $\tilde{\mathbf{E}}$ therein as $\tilde{\mathbf{E}} = \mathbf{V}_K \tilde{\mathbf{V}}_K^\top - \tilde{\mathbf{S}}_K \tilde{\mathbf{S}}_K^\top$. Precisely, this entails

$$\sqrt{F(\tilde{\mathcal{C}}_1, \dots, \tilde{\mathcal{C}}_K)} - \sqrt{(1+\epsilon)F^*} \leq (2+\epsilon)\|\tilde{\mathbf{E}}\|_F. \tag{80}$$

Next, we bound $\|\tilde{\mathbf{E}}\|_F$. Applying Lemma 4 and using the triangle inequality we get that

$$\begin{aligned}
\|\tilde{\mathbf{E}}\|_F &\leq \sqrt{2K} \|\mathbf{V}_K \tilde{\mathbf{V}}_K^\top - \tilde{\mathbf{S}}_K \tilde{\mathbf{S}}_K^\top\|_2 \\
&\leq \sqrt{2K} (\|\mathbf{V}_K \tilde{\mathbf{V}}_K^\top - \tilde{\mathbf{V}}_K \tilde{\mathbf{V}}_K^\top\|_2 + \|\tilde{\mathbf{V}}_K \tilde{\mathbf{V}}_K^\top - \tilde{\mathbf{S}}_K \tilde{\mathbf{S}}_K^\top\|_2),
\end{aligned}$$

Moreover, Proposition 1 implies that

$$\|\mathbf{V}_K \tilde{\mathbf{V}}_K^\top - \tilde{\mathbf{V}}_K \tilde{\mathbf{V}}_K^\top\|_2 \leq \sqrt{\tilde{\gamma}/(1+\tilde{\gamma})} \tag{81}$$

Our remaining task is to bound $\|\tilde{\mathbf{V}}_K \tilde{\mathbf{V}}_K^\top - \tilde{\mathbf{S}}_K \tilde{\mathbf{S}}_K^\top\|_2$. Observe that

$$\|\tilde{\mathbf{V}}_K \tilde{\mathbf{V}}_K^\top - \tilde{\mathbf{S}}_K \tilde{\mathbf{S}}_K^\top\|_2 = \|\tilde{\mathbf{S}}_{R-K}^\top \tilde{\mathbf{V}}_K\|_2, \tag{82}$$

$$\sigma_K(\tilde{\mathbf{S}}^*) \geq \sigma_K(\tilde{\mathcal{H}}(\mathbf{S})\mathbf{B}) - \|\tilde{\Delta}\|_2, \tag{83}$$

where we recalled the definition $\tilde{\Delta} = \tilde{\mathbf{S}}^* - \tilde{\mathcal{H}}(\mathbf{S})\mathbf{B}$ and applied the Weyl's inequality [49]. From (41), we have that

$$\sigma_K(\tilde{\mathcal{H}}(\mathbf{S})\mathbf{B}) - \|\tilde{\Delta}\|_2 = \sigma_{K+1}(\tilde{\mathcal{H}}(\mathbf{S})\mathbf{B}) + \tilde{\delta}, \tag{84}$$

with $\tilde{\delta} > 0$. Finally, applying the Wedin theorem [53] yields

$$\|\tilde{\mathbf{S}}_{R-K}^\top \tilde{\mathbf{V}}_K\|_2 \leq (\tilde{\delta})^{-1} \|\tilde{\Delta}\|_2. \tag{85}$$

REFERENCES

[1] H.-T. Wai, S. Segarra, A. E. Ozdaglar, A. Scaglione, and A. Jadbabaie, "Community detection from low-rank excitations of a graph filter," in *Proc ICASSP*, April 2018.

[2] A. Sandryhaila and J. M. Moura, "Discrete signal processing on graphs," *IEEE Trans. Signal Process.*, vol. 61, no. 7, pp. 1644–1656, 2013.

[3] D. Shuman, S. Narang, P. Frossard, A. Ortega, and P. Vandergheynst, "The emerging field of signal processing on graphs: Extending high-dimensional data analysis to networks and other irregular domains," *IEEE Signal Process. Mag.*, vol. 30, no. 3, pp. 83–98, May 2013.

[4] A. Ortega, P. Frossard, J. Kovačević, J. M. Moura, and P. Vandergheynst, "Graph signal processing," *arXiv preprint arXiv:1712.00468*, 2017.

[5] A. G. Marques, S. Segarra, G. Leus, and A. Ribeiro, "Sampling of graph signals with successive local aggregations," *IEEE Trans. Signal Process.*, vol. 64, no. 7, pp. 1832–1843, April 2016.

[6] S. Chen, R. Varma, A. Sandryhaila, and J. Kovačević, "Discrete signal processing on graphs: Sampling theory," *IEEE Trans. Signal Process.*, vol. 63, no. 24, pp. 6510–6523, Dec 2015.

[7] D. Romero, M. Ma, and G. B. Giannakis, "Kernel-based reconstruction of graph signals," *IEEE Trans. Signal Process.*, vol. 65, no. 3, pp. 764–778, Feb 2017.

[8] S. Segarra, A. G. Marques, G. Leus, and A. Ribeiro, "Reconstruction of graph signals through percolation from seeding nodes," *IEEE Trans. Signal Process.*, vol. 64, no. 16, pp. 4363–4378, Aug 2016.

[9] S. Segarra, A. G. Marques, and A. Ribeiro, "Optimal graph-filter design and applications to distributed linear network operators," *IEEE Trans. Signal Process.*, vol. 65, no. 15, pp. 4117–4131, Aug 2017.

[10] E. Isufi, A. Loukas, A. Simonetto, and G. Leus, "Autoregressive moving average graph filtering," *IEEE Trans. Signal Process.*, vol. 65, no. 2, pp. 274–288, Jan 2017.

[11] J. Friedman, T. Hastie, and R. Tibshirani, "Sparse inverse covariance estimation with the graphical lasso," *Biostatistics*, vol. 9, no. 3, pp. 432–441, 2008.

[12] E. Pavez and A. Ortega, "Generalized Laplacian precision matrix estimation for graph signal processing," in *IEEE Intl. Conf. Acoust., Speech and Signal Process. (ICASSP)*, Shanghai, China, Mar. 20–25, 2016.

[13] Y. Shen, B. Baingana, and G. B. Giannakis, "Kernel-based structural equation models for topology identification of directed networks," *IEEE Trans. Signal Process.*, vol. 65, no. 10, pp. 2503–2516, 2017.

[14] X. Cai, J. A. Bazerque, and G. B. Giannakis, "Sparse structural equation modeling for inference of gene regulatory networks exploiting genetic perturbations," *PLoS Computational Biology*, Jun. 2013.

[15] H.-T. Wai, A. Scaglione, U. Harush, B. Barzel, and A. Leshem, "Rids: Robust identification of sparse gene regulatory networks from perturbation experiments," *arXiv preprint arXiv:1612.06565*, 2016.

[16] X. Dong, D. Thanou, P. Frossard, and P. Vandergheynst, "Learning Laplacian matrix in smooth graph signal representations," *IEEE Trans. Signal Process.*, vol. 64, no. 23, pp. 6160–6173, Dec 2016.

[17] V. Kalofolias, "How to learn a graph from smooth signals," in *Intl. Conf. Artif. Intel. Stat. (AISTATS)*. J. Mach. Learn. Res., 2016, pp. 920–929.

[18] S. P. Chepuri, S. Liu, G. Leus, and A. O. Hero, "Learning sparse graphs under smoothness prior," in *IEEE Intl. Conf. Acoust., Speech and Signal Process. (ICASSP)*, March 2017, pp. 6508–6512.

[19] S. Segarra, A. G. Marques, G. Mateos, and A. Ribeiro, "Network topology inference from spectral templates," *IEEE Trans. Signal and Info. Process. over Networks*, vol. 3, no. 3, pp. 467–483, 2017.

[20] S. Segarra, G. Mateos, A. G. Marques, and A. Ribeiro, "Blind identification of graph filters," *IEEE Trans. Signal Process.*, vol. 65, no. 5, pp. 1146–1159, March 2017.

[21] R. Shafipour, S. Segarra, A. G. Marques, and G. Mateos, "Network topology inference from non-stationary graph signals," in *Proc. ICASSP*, March 2017, pp. 5870–5874.

[22] H.-T. Wai, A. Scaglione, and A. Leshem, "Active sensing of social networks," *IEEE Trans. Signal and Info. Process. over Networks*, vol. 2, no. 3, pp. 406–419, 2016.

[23] D. Marbach, J. C. Costello, R. Küffner, N. M. Vega, R. J. Prill, D. M. Camacho, K. R. Allison, A. Aderhold, R. Bonneau, Y. Chen *et al.*, "Wisdom of crowds for robust gene network inference," *Nature methods*, vol. 9, no. 8, p. 796, 2012.

[24] S. Fortunato, "Community detection in graphs," *Physics reports*, vol. 486, no. 3, pp. 75–174, 2010.

[25] O. Candogan, K. Bimpikis, and A. Ozdaglar, "Optimal pricing in networks with externalities," *Operations Research*, vol. 60, no. 4, pp. 883–905, 2012.

[26] B. Ata, A. Belloni, and O. Candogan, "Latent agents in networks: Estimation and pricing," *arXiv:1808.04878v1*, August 2018.

[27] M. H. DeGroot, "Reaching a consensus," *Journal of the American Statistical Association*, vol. 69, no. 345, pp. 118–121, 1974.

[28] U. von Luxburg, "A tutorial on spectral clustering," *Statistics and Computing*, vol. 17, no. 4, pp. 395–416, Dec 2007.

[29] J. A. Hartigan and M. A. Wong, "Algorithm AS 136: A k-means clustering algorithm," *Journal of the Royal Statistical Society. Series C (Applied Statistics)*, vol. 28, no. 1, pp. 100–108, 1979.

[30] S. Dasgupta, *The hardness of k-means clustering*. Department of CSE, University of California, San Diego, 2008.

[31] A. Kumar, Y. Sabharwal, and S. Sen, "A simple linear time $(1+\epsilon)$ -approximation algorithm for k-means clustering in any dimensions," in *FOCS*. IEEE, 2004, pp. 454–462.

[32] J. Tsitsiklis, "Problems in decentralized decision making and computation," Ph.D. dissertation, Dept. of Electrical Engineering and Computer Science, M.I.T., Boston, MA, 1984.

[33] D. P. Bertsekas, *Nonlinear programming*. Athena scientific Belmont, 1999.

[34] C. Boutsidis, P. Kambadur, and A. Gittens, "Spectral clustering via the power method-provably," in *International Conference on Machine Learning*, 2015, pp. 40–48.

[35] R. Vershynin, *High-Dimensional Probability*. Cambridge University Press, 2017.

[36] A. Agarwal, S. Negahban, and M. J. Wainwright, "Noisy matrix decomposition via convex relaxation: Optimal rates in high dimensions," *The Annals of Statistics*, pp. 1171–1197, 2012.

[37] J. Huang, T. Zhang, and D. Metaxas, "Learning with structured sparsity," *JMLR*, vol. 12, no. Nov, pp. 3371–3412, 2011.

[38] S. N. Negahban, P. Ravikumar, M. J. Wainwright, and B. Yu, "A unified framework for high-dimensional analysis of m-estimators with decomposable regularizers," *Statistical Science*, pp. 538–557, 2012.

[39] P. W. Holland, K. B. Laskey, and S. Leinhardt, "Stochastic blockmodels: First steps," *Social networks*, vol. 5, no. 2, pp. 109–137, 1983.

[40] D. Acemoglu, A. Ozdaglar, and A. ParandehGheibi, "Spread of (mis) information in social networks," *Games and Economic Behavior*, vol. 70, no. 2, pp. 194–227, 2010.

[41] E. Yıldız, A. Ozdaglar, D. Acemoglu, A. Saberi, and A. Scaglione, "Binary opinion dynamics with stubborn agents," *ACM Transactions on Economics and Computation (TEAC)*, vol. 1, no. 4, p. 19, 2013.

[42] P. Jia, A. MirTabatabaei, N. E. Friedkin, and F. Bullo, "Opinion dynamics and the evolution of social power in influence networks," *SIAM review*, vol. 57, no. 3, pp. 367–397, 2015.

[43] M. E. Yıldız and A. Scaglione, "Computing along routes via gossiping," *IEEE Trans. on Signal Process.*, vol. 58, no. 6, pp. 3313–3327, 2010.

[44] F. D. Malliaros and M. Vazirgiannis, "Clustering and community detection in directed networks: A survey," *Physics Reports*, vol. 533, no. 4, pp. 95–142, 2013.

[45] J. S. Coleman *et al.*, "Introduction to mathematical sociology." *Introduction to mathematical sociology*, 1964.

[46] A. L. Traud, P. J. Mucha, and M. A. Porter, "Social structure of Facebook networks," *Physica A: Statistical Mechanics and its Applications*, vol. 391, no. 16, pp. 4165–4180, 2012.

[47] A. Aravkin, S. Becker, V. Cevher, and P. Olsen, "A variational approach to stable principal component pursuit," in *UAI*, July 2014.

[48] A. Gittens, P. Kambadur, and C. Boutsidis, "Approximate spectral clustering via randomized sketching," *arXiv:1311.2854v1*, 2013.

[49] G. H. Golub and C. F. Van Loan, *Matrix computations*. JHU Press, 2012, vol. 3.

[50] C. Davis and W. M. Kahan, "The rotation of eigenvectors by a perturbation. iii," *SIAM Journal on Numerical Analysis*, vol. 7, no. 1, pp. 1–46, 1970.

[51] R. Vershynin, "How close is the sample covariance matrix to the actual covariance matrix?" *Journal of Theoretical Probability*, vol. 25, no. 3, pp. 655–686, 2012.

[52] J. A. Tropp, "User-friendly tail bounds for sums of random matrices," *Foundations of computational mathematics*, vol. 12, no. 4, pp. 389–434, 2012.

[53] P.-A. Wedin, "Perturbation bounds in connection with singular value decomposition," *BIT Numerical Mathematics*, vol. 12, no. 1, pp. 99–111, 1972.